

THE UNIVERSITY OF MICHIGAN  
COLLEGE OF ENGINEERING  
Department of Aerospace Engineering

Technical Report

HYDROMAGNETIC KELVIN-HELMHOLTZ INSTABILITY  
IN SHEAR LAYERS OF NON-ZERO THICKNESS

R.S.B. Ong  
N. F. Roderick

ORA Project 085810

supported by:

U. S. AIR FORCE  
OFFICE OF SCIENTIFIC RESEARCH  
GRANT NO. AF-AFOSR-825-67  
ARLINGTON, VIRGINIA

administered through:

OFFICE OF RESEARCH ADMINISTRATION      ANN ARBOR

May 1971

This report was also a dissertation submitted in partial fulfillment of the requirements for the degree of Doctor of Philosophy in The University of Michigan, 1971.

## TABLE OF CONTENTS

	Page
LIST OF FIGURES	iv
LIST OF SYMBOLS	v
I. INTRODUCTION	1
II. REVIEW OF PREVIOUS WORK	8
III. THE TWO FLUID MODEL AND THE EQUIVALENT DIELECTRIC TENSOR	19
IV. DISPERSION RELATION AND SOLUTIONS	39
V. SINGLE FLUID EQUATIONS AND FINITE THICKNESS MODEL	49
VI. INCOMPRESSIBLE FLOW LIMIT	57
VII. EFFECTS OF COMPRESSIBILITY	71
VIII. SUMMARY AND CONCLUSIONS	83
REFERENCES	89
APPENDIX	94

## LIST OF FIGURES

	Page
Figure 1. Magnetosphere Model	2
Figure 2. Inhomogeneous Slab Shear Layer Model	20
Figure 3. Growth Rate vs Wave Number Ratio. Effects of Velocity Shear	45
Figure 4. Growth Rate vs Wave Number Ratio. Effects of Local Shear Flow Speed	46
Figure 5. Growth Rate vs Wave Number Ratio. Effects of Density Gradients	47
Figure 6. Finite Thickness Shear Layer Model	52
Figure 7. Growth Rate vs Wave Number. Effects of Finite Thickness and Parallel Magnetic Field	67
Figure 8. Neutral Stability Wave Number. Effects of Parallel Magnetic Field	69
Figure 9. Growth Rate vs Wave Number. Effects of Finite Thickness and Compressibility	78
Figure 10. Neutral Stability. Effects of Compressibility and Transverse Magnetic Field	80
Figure A-1. Growth Rate vs Wave Number. Exact Solution for no Magnetic Field Inside the Layer	97

## LIST OF SYMBOLS

$A$	Alfven Mach number
$\vec{B}$	magnetic field
$B_0$	equilibrium magnetic field
$b$	perturbation magnetic
$C_A$	Alfven speed based on the y-component of the magnetic field
$C_M$	magnetoacoustic speed
$C_s$	adiabatic sound speed
$c_A$	Alfven speed based on the z-component magnetic field
$\vec{D}$	displacement current
$d$	half thickness of the shear layer
$\vec{E}$	electric field
$e$	electron charge
$\hat{e}$	unit vector
$\vec{H}$	magnetic field intensity
$J$	current density
$\vec{K}$	equivalent dielectric tensor
$\vec{k}$	wave vector
$k$	nondimensional wave number
$k_c$	critical nondimensional wave number
	Boltzmann's constant
$L$	gradient length scale
$\ell$	characteristic length of perturbation
$M$	ion mass
$m$	electron mass
$n$	number density
$m$	magnetoacoustic Mach number
$m$	electron mass
$n$	number density

$p$	pressure
$R$	gas constant
$R_E$	radius of the earth
$T$	temperature
$t$	time
$U_a$	ion acoustic speed
$U_e$	electron sound speed
$U_i$	ion sound speed
$U_p$	plasma sound speed
$V$	Galilean transformed equilibrium velocity
$\vec{v}$	velocity
$W$	Doppler shifted frequency
$\vec{x}$	Cartesian coordinate vector
$\beta$	ratio of plasma pressure to magnetic pressure
$\Gamma$	nondimensional growth rate
$\gamma$	growth rate
$\tilde{\gamma}$	ratio of specific heats
$\epsilon_0$	dielectric constant of free space
$\eta$	$(1/n_0)(dn_0/dx)$
$\kappa$	ratio of y wave number to z wave number
$\kappa_B$	$(1/B_0)(dB_0/dx)$
$\Lambda$	ratio of $\eta$ to z wave number
$\Lambda_\sigma$	$(1/k_z)(1/v_{OZ})(dv_{OZ}/dx)$
$\lambda_{De}$	Debye length
$\mu_0$	Permeability of free space
$\nu$	ratio of perturbation number density to equilibrium number density
$\rho$	mass density
$\rho_c$	charge density

$\vec{\sigma}$	conductivity tensor
$\sigma$	ratio of local shear flow speed to local Alfvén speed
$\phi$	electric potential
$\psi$	nondimensional frequency
$\Omega$	nondimensional frequency
$\Omega_i$	ion cyclotron frequency
$\Omega_R$	real part of $\Omega$
$\omega$	frequency

### Subscripts

0	equilibrium state
1	perturbation state
e	electrons
i	ions
x	x-component
y	y-component
z	z-component

## I. INTRODUCTION

The development of instabilities in parallel fluid flows with a velocity gradient is well known (11, p. 481). The instability arises because of the relative velocity between fluid layers. This instability was first studied by Helmholtz and Lord Kelvin in the last century, and has become known as the Kelvin-Helmholtz (K-H) instability. While the original work dealt with the instability of heterogeneous layers of fluid separated by a tangential velocity discontinuity, Rayleigh (50) studied the effects of a finite shear layer thickness on the hydrodynamic problem.

In many physical situations conditions are such that a velocity shear exists in a plasma or a magnetohydrodynamic (MHD) fluid. Here the behavior of the physical system is modified by the presence of electromagnetic fields. Our primary interest has been motivated by one such physical situation, the flow stability at the magnetopause or boundary between the post shock solar wind flow and the earth's magnetosphere. The physical situation of the solar wind flow around the earth is shown in Fig. 1. The supersonic solar wind is slowed and compressed by the earth's bow shock and then flows around the earth's magnetospheric cavity. The earth's dipole magnetic field is compressed and distorted by the solar wind plasma. The stronger



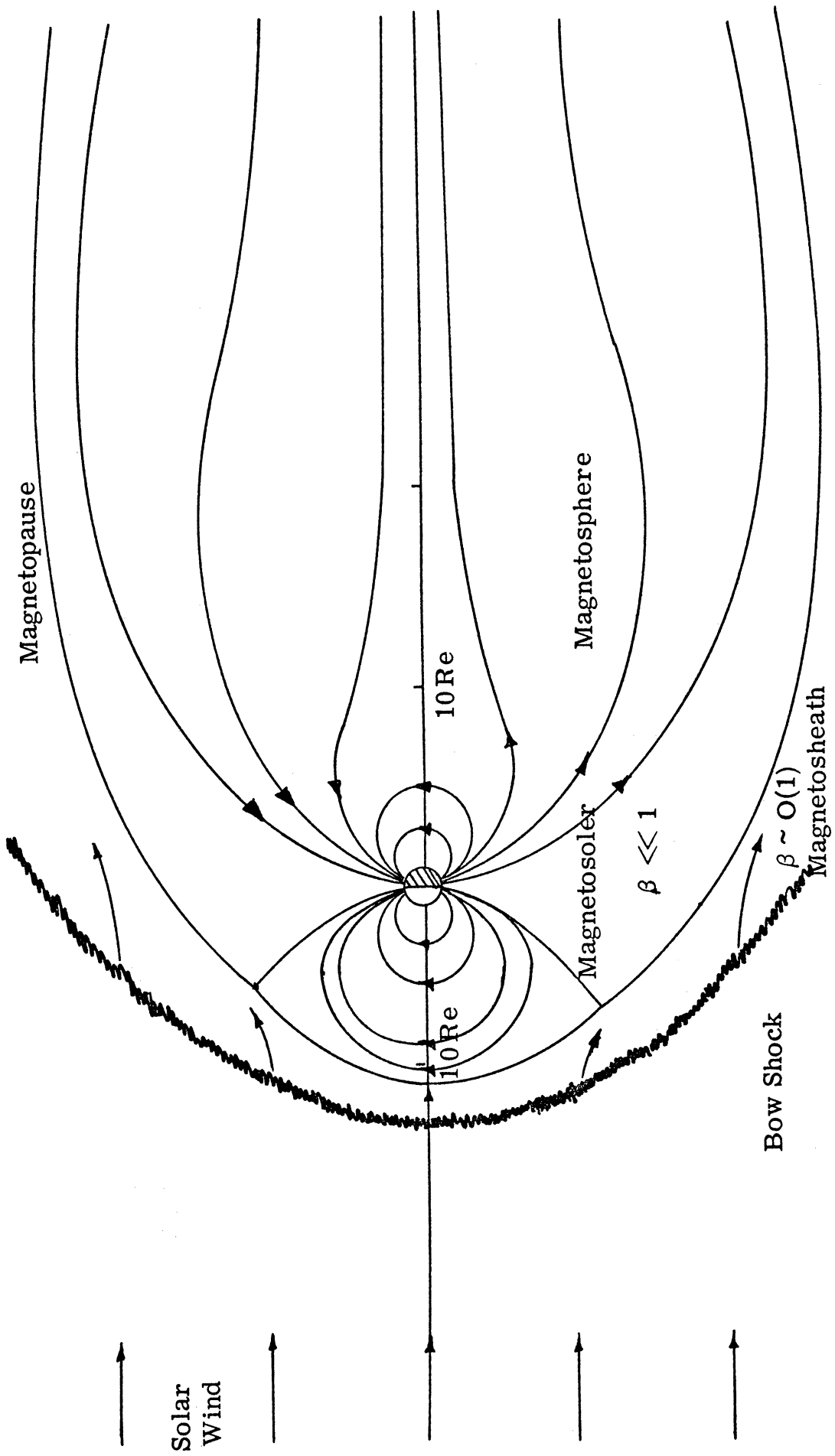


Figure 1. Magnetosphere Model

magnetic field of the dipole deflects the solar wind plasma and in the equilibrium configuration prevents the solar wind plasma from entering the magnetosphere. A region of velocity shear exists at this boundary, the magnetopause. At large distances this shear region appears to be a tangential velocity discontinuity between the magnetosheath, post shock solar wind flow, and the nearly stationary magnetospheric plasma. This region is one in which a possible hydro-magnetic Kelvin-Helmholtz instability may exist. Investigations along these lines have been carried out by many authors treating the magnetopause as a tangential velocity discontinuity. Southwood (61) and MacKenzie (40) have been two of the latest investigators, and their papers contain references to much of the earlier work. The hydro-magnetic Kelvin-Helmholtz instability has been discussed in conjunction with the interaction between the solar wind and the magnetosphere (4) and to explain the semiannual variation of the earth's geomagnetic cavity (7). Although this will be our primary area of concern some of the results obtained will be applicable to other plasma problems where a velocity shear may affect the flow field.

Among the many other physical situations with velocity shear are the regions between fast and slow streams of particles in the solar wind (13, 32), the behavior of plasmas contained in experimental devices such as Q machines (14, 15, 31) and the flow in MHD boundary layers and wakes (37-39, 24-26, 49).

In all of these problems a parameter of primary concern is the plasma  $\beta$ . We define  $\beta$  as the ratio of the plasma kinetic pressure  $p$  to the magnetic pressure due to the magnetic field,  $B$ . In MKS units this gives

$$\beta = \frac{p}{B^2/2\mu_0}. \quad (1.1)$$

$\mu_0$  is the permeability of free space. For  $\beta < 1$  we have a physical situation in which the plasma may be confined by the magnetic field while for  $\beta > 1$  confinement is not possible. For the magnetopause problem the range of  $\beta$  is shown in Fig. 1. Outside of the magnetosphere the plasma streams through space with  $\beta \geq O(1)$ . Inside the magnetosphere where the geomagnetic field is large we have  $\beta \ll 1$ . For the case of a confined plasma both in the laboratory and in space we generally have  $\beta \ll 1$  as is the case with the magnetospheric plasma. This case in general allows simplification in the mathematics for dealing with plasma problems. This simplification occurs because  $\beta \ll 1$  usually allows the problem to be treated in the electrostatic approximation,  $\vec{E} = -\nabla\phi$  where  $\vec{E}$  is the electric field and  $\phi$  the electric potential (63, p. 25)<sup>1</sup>. For this case magnetic field fluctuations are not considered in treating wave propagation and stability problems.

<sup>1</sup>For two more general discussions of the applicability of the electrostatic approximation to  $\beta \ll 1$  problems see Montgomery (46).

For the magnetopause problem, however, this is not the case. The presence of the  $\beta > 1$  region in the magnetosheath means that the electrostatic approximation cannot be made in this problem. For this case we must account for fluctuations in the magnetic field.

Before discussing the stability of the magnetopause, let us review some of the physical aspects of the boundary and the flow field. A general review of the interaction of the solar wind with the earth's magnetic field can be found in Scarf (54), the Reviews of Geophysics (51), and Wolfe and Intriligator (72) among others. Physical parameters are shown in Fig. 1. On the magnetosheath side of the boundary the solar wind plasma temperature is  $10^6$  °K and the number density is the order of 10 ion-electron pair per cubic centimeter. The flow in the magnetosheath is highly turbulent with fluctuations in both the magnitude and direction of the magnetic fields in the  $30\gamma$  to  $40\gamma$  range ( $1\gamma = 10^{-5}$  gauss =  $10^{-9}$  Webers/m<sup>2</sup>). The magnetosheath field is frequently directed southward (29, p. 302). For this region  $\beta \gtrsim 1$ . The flow velocity is zero at the subsolar point and increases as one moves away from this point along the boundary in any direction.

Inside the magnetosphere the plasma density is of the order of  $10^{-1}$  ion-electron pair per cubic centimeter at a temperature of around  $10^5$  °K -  $10^6$  °K (40). Inside the boundary the magnetic field

strength is of the order of  $50\gamma - 100\gamma$ . The field here is nearly constant in both magnitude and direction. These conditions give  $\beta \ll 1$ . Recent investigations by Smith and Davis (60) show an additional amount of spread in these data with nearly equal field magnitudes in the magnetosheath and magnetosphere on certain boundary crossings. These measurements also show the absence of any significant magnetic field component normal to the interface indicating a closed magnetosphere and a tangential magnetic discontinuity at large length scales. Inside the magnetosphere the plasma is essentially at rest. For large length scales the magnetopause thus represents a tangential velocity and magnetic field discontinuity. This will be true for both "open" or "closed" magnetosphere model for the low latitude equatorial regions and for the high latitude regions for a "closed" magnetosphere. The applicability of a surface discontinuity model to the high latitudes for an "open" magnetosphere is certainly questionable as has been discussed by Southwood (61).

While at large length scales the magnetopause appears as a velocity discontinuity, at smaller scales the thickness is non-zero. Simple particle reflection theory indicates a magnetopause thickness in the 150 km to 200 km range for 1 Kev protons and magnetosphere strengths of the order of  $50\gamma$  (29, p. 300). This corresponds to the

ion Larmor radius ( $a_i = U_i / \Omega_i$ ) for a 1 Kev solar wind proton entering the magnetospheric field at right angles. It is considerably less than the Larmor radius of a magnetospheric proton in the same field. In the above  $U_i$  is the ion sound speed  $U_i = \gamma (k/M) T_i$  and  $\Omega_i$  is the ion cyclotron frequency  $\Omega_i = eB/M$ . Satellite data (29, p. 301) indicates the thickness to be of the order of 100 km or greater. This distance represents a lower limit and may be larger due to the motion of the magnetopause. Such motions have been observed with velocities in the 50 km/sec to 150 km/sec range (60). The motion appears to be quasisinusoidal with peak amplitudes of  $1/3 R_e$  ( $R_e = 1$  earth radii) and a period of approximately 2 minutes. Wave motion has also been detected both inside and outside the boundary. This appears to be associated with the boundary motion (2, 20).

## II. REVIEW OF PREVIOUS WORK

A general review of the K-H problem in both ordinary fluid mechanics and in magnetohydrodynamics can be found in Chandrasekhar (11, p. 481), Drazin and Howard (16), and Gerwin (23). The material in Chandrasekhar covers work prior to 1960, that in Drazin and Howard work on inviscid parallel shear flows prior to 1966, and that in Gerwin work on the K-H problem in hydrodynamics, MHD, and plasmas prior to 1968. The work we shall consider here will be primarily that which is relevant to the magnetopause problem. This work, in general, falls into the class of low frequency linear stability analysis using the hydromagnetic equations.

In studying the stability of the magnetopause, the general method has been to investigate the behavior of an interface of zero thickness between two hydromagnetic fluids in relative motion. The effects of gravitational forces and the curvature of the boundary are neglected. The general formulation for arbitrary tangential magnetic fields and relative velocities leads to a tenth degree dispersion relation (61). Using the hydromagnetic equations with infinite conductivity, Syrovatskii (66), Chandrasekhar (11), and Axford (3, 5) discussed the incompressible problem while Sen (56),

Fejer (22), Lerche (36), Southwood (61) and MacKenzie (40) included the effects of compressibility. With the exception of Southwood, all of the above introduce a number of simplifying assumptions to reduce the degree of the dispersion relation. Southwood maintained a general formulation and studied the onset of instability. Both he and MacKenzie used satellite data to obtain stability conditions at the interface. The conclusions of the above work can be summarized by saying that the hydromagnetic equivalent of the Kelvin-Helmholtz instability does exist for zero thickness shear layers. These results have shown that compressibility tends to stabilize the interface but that the effect of the magnetic field can be either stabilizing or destabilizing (22). In application to the magnetopause problem MacKenzie (40) has shown that the high latitude regions near the earth are stable in the quiet solar wind when pre-shock velocities are of the order of 400 km/sec. At most the extreme reaches the tail is unstable at these times. For "gusty" days when the pre-shock velocity reaches velocities near 700 km/sec the region of instability moves in close to the earth at high latitudes. Southwood (61) has shown that at low latitudes, in the equatorial region, where the flow velocity has a large component perpendicular to the geomagnetic field, the hydromagnetic K-H instability will develop if a critical magnetosheath velocity is exceeded. As one moves from



the subsolar point toward dawn or dusk, the magnetosheath velocity increases and instability is possible. The onset of instability occurs for the lowest velocity when the magnetosheath field is parallel or antiparallel to the geomagnetic field, i. e. northward or southward. Southwood has also shown that the fastest growing modes will be closely aligned to a plane perpendicular to the earth's field and that the waves will circularly polarize.

Hans (28) has used the finite ion Larmor radius expansion to the fluid equations to investigate the effects of finite Larmor radii and collisional effects on the zero thickness incompressible hydromagnetic problem. For a constant transverse magnetic field and wave propagation parallel to the flow velocity, he has found that the effects of the finite ion Larmor radius stabilized the flow and that collisional effects if small provided stabilization but if larger than a critical value were destabilizing.

Talwar (67) and more recently Duhau et al (18) have extended the above work to collisionless plasmas with non-isotropic pressure tensors. These authors utilized the collisionless Chew-Goldberger-Low (CGL) equations (12) to investigate the hydromagnetic stability of a non-isotropic plasma with a tangential velocity discontinuity. Their results were calculated for the special case of uniform magnetic field with propagation parallel to the field. These results

show that the instability does exist and that changes in isotropy do not in general effect the problem.

The presence of the hydromagnetic Kelvin-Helmholtz instability provides a mechanism for providing a viscous interaction between the solar wind and the magnetosphere. Such a viscous interaction has been proposed by Axford and Hines (4) and others to explain magnetospheric convection and certain auroral phenomena. It should be noted that the viscous interaction associated with the Kelvin-Helmholtz instability may be only one of many processes occurring at the boundary to produce the total viscous drag. Among other possible mechanisms are the viscous interaction of Axford and Hines (4) fast field line merging of Dungey (19), Brice (9) and others; and ion cyclotron damping based on a homogeneous plasma model of Eviatar and Wolf (21).

Physical evidence in the form of satellite and ground based observations of magnetic fields has also been presented for the existence of the hydromagnetic Kelvin-Helmholtz instability at the magnetopause. Most of this evidence has been summarized by Dungey and Southwood (20). A brief outline of this work will be presented here along with other work published since the above paper appeared. As mentioned previously satellite observations show multiple crossings of the magnetopause indicating quasisinusoidal

oscillations and the presence of waves on the boundary. Observations of this nature have been made by Anderson et al (1), Aubrey et al (2), Smith and Davis (60), and others (see Ref. 20). The oscillations are in the low frequency range with periods of the order of 10 sec to 10 min. The recent results of Aubrey et al indicated these waves travel tailward along the magnetopause with a velocity of the same order as the magnetosheath plasma flow velocity. These results are consistent in frequency range and convection velocity with waves produced by the Kelvin-Helmholtz instability of the boundary (2, 20). Additional data from Greenstadt (27) and Kaufmann and Konradi (34) indicated the presence of large amplitude waves inside the magnetosphere adjacent to the boundary as well as outside the boundary in the magnetosheath. Wave periods were in the 10 sec to 10 min range again and consistent with Kelvin-Helmholtz theory. Kaufmann and Konradi indicated some of the magnetosheath waves originated at the magnetopause and were attributable to boundary motion. Dungey and Southwood have correlated the wave magnetic field oscillation and polarization from Explorer 33 data with that predicted by Southwood's hydromagnetic Kelvin-Helmholtz instability theory. These data showed a reversal in wave polarization as the boundary was crossed in agreement with the theory. Other satellite

and ground based data on magnetosphere waves and magnetic field pulsations summarized by Dungey and Southwood also showed ultra low frequency pulsations in the pc 2 (5-10 sec period) to pc 5 (150-600 sec period) range. The pulsations often agreed in the sense of rotation and polarization with surface waves on the magnetopause. Sen (57, 58) has also correlated micropulsation data with Kelvin-Helmholtz instability theory and found the results consistent. The diurnal variation of the continuous pulsations is also explained by the Kelvin-Helmholtz theory (20) as is the more recent explanation of the semiannual variation of geomagnetic activity given by Boller and Stotlow (7). There thus appears to be strong evidence for the presence of the hydromagnetic Kelvin-Helmholtz instability of the magnetopause.

All of the above mentioned theoretical work on the hydromagnetic Kelvin-Helmholtz instability suffers from one drawback, however, as was pointed out by Lerche (36). In the velocity discontinuity models used above the largest growth rates, those which will govern the physical behavior of the interface, occur for the largest wave numbers. The growth rate increases indefinitely with wave number. Thus while the theory assumes that all length scales of physical interest are much larger than the thickness of the shear layer, the largest growth rates occur for wavelengths approaching zero. In

this manner the formulation of the problem is inconsistent. Clearly to obtain a consistent formulation the thickness of the layer must be taken into account even in the hydromagnetic formulation. In addition to the layer thickness Lerche mentions other length scales such as the ion Larmor radius and the Debye length defined as

$$\lambda_{De}^2 = \frac{\epsilon_0 k T_e}{n_e e^2}.$$

At these length scales the hydromagnetic formulation must be abandoned because of wave-particle interactions and kinetic theory must be used. Because of the above inconsistency and the failure to include layer thickness, ion cyclotron radius and possibly smaller length scales, Lerche argues that the hydromagnetic formulation is not valid and that a kinetic theory formulation is required to properly discuss the problem of magnetopause stability.

A similar situation occurs in ordinary hydrodynamics. For this case, too, the growth rate increases with wave number for shear layers of zero thickness (11, p. 484). Here, however, when the thickness of the layer is taken into account, the growth rate remains finite and is zero for wave numbers beyond a critical value. This result was obtained originally by Rayleigh (50) for incompressible flow with a

linear velocity profile. The wave number for zero growth rate,  $k_c$ , is given by the solution of the transcendental equation

$$2k_c = 1 + e^{-2k_c d}$$

$$k_c = k_{zc} d$$

where  $d$  is the half thickness of the layer. Recently Schuurman (55) has included compressibility in the finite thickness linear velocity profile and has shown that the first effects of compressibility provide flow stabilization. This is in agreement with the earlier zero thickness work of Miles (44). Stabilization at large wave numbers has been obtained for other continuous shear layers such as the incompressible hyperbolic tangent shear layer investigated numerically by Michalke (43). A similar hydromagnetic problem has also been studied by Gotoh (24, 25) and Gotoh and Namata (26). They considered an incompressible hydromagnetic free boundary layer with a hyperbolic tangent velocity profile and a constant magnetic field parallel to the flow velocity. Gotoh initially obtained approximate results for long wave lengths and growth rates near zero. Later he was able to numerically obtain solutions for the wave number of neutral disturbances. In the high Reynolds number and high magnetic Reynolds number case these results indicated a critical upper limit on the wave number where the growth rate became zero. They also indicated a stabilizing effect for a parallel magnetic field. No quantitative results were obtained for other wave numbers or larger growth rates.

Another analogous situation also occurs in the study of the Kelvin-Helmholtz instability in low  $\beta$  plasmas. Using a two fluid hydromagnetic approach for a nonuniform infinite plasma slab with a constant magnetic field, D'Angelo (14) found that instability developed for shear velocity changes of the order of the ion thermal speed. Melchior and Popovic (42) extended this work to include the effects of the finite ion Larmor radius (FLR) and Smith and von Goeler (59) treated the problem using the Vlasov-equation to describe the ion motion and the electron fluid equations to describe the electrons. Recently Baikov (6) has extended this work to include temperature gradients using the two fluid equations. In all of this work as the wave numbers becomes smaller, such that the plasma becomes more homogeneous with respect to the perturbation wavelength, the growth rates become zero.

In both the finite thickness hydrodynamic problem and the infinite plasma slab problem the effects of non-zero shear layer thickness resulted in stabilization of the disturbances. For this reason and because of the strong experimental evidence of the existence of the hydromagnetic Kelvin-Helmholtz instability at the magnetopause, we will further consider the effect of non-zero shear layer thickness on the hydromagnetic problem. While we agree with Lerche that a

complete investigation should involve a kinetic theory treatment, we also accept his observation that such a treatment must be based on a detailed knowledge of the equilibrium distribution function for this problem. At present, as at the time of Lerche's observation, such detailed knowledge does not exist. Thus like Southwood (61), while acknowledging the limitations of the hydromagnetic theory we will formulate the problem in this limit, utilizing the fluid equations, and considering velocity shear layers of non-zero thickness. While not providing a completely detailed description of the hydromagnetic Kelvin-Helmholtz instability to all length and time scales, such a formulation should lead to a better understanding of the nature of Lerche's inconsistency as related to the hydromagnetic assumption and the overall behavior of the boundary.

The models we use in this study will employ the hydromagnetic equations as already discussed. We shall also assume the existence of an equilibrium magnetopause which will be perturbed to study the stability of the layer. We shall not enter into a discussion of the existence of such a layer (10, 33). Similarly while the plasma will be taken to be collisionless we will assume that sufficient wave particle interactions take place in the turbulent magnetosheath to insure that the distribution function remains near Maxwellian so that the fluid equations are applicable in the low frequency regime. Our



aim again is not to develop a complete theory for the magnetopause and its stability but to investigate the effect of non-zero shear layer thickness on the hydromagnetic model.

We begin by studying the hydromagnetic Kelvin-Helmholtz instability in an infinite inhomogeneous plasma slab using the hydromagnetic two fluid model. This model neglects edge effects and extends the electrostatic,  $\beta \ll 1$ , work of D'Angelo to the  $\beta \sim O(1)$  region with a nonuniform magnetic field. After this we employ the single fluid hydromagnetic equations to study the effects of finite shear layer thickness. As in previous work (14, 40, 61) we will consider a cartesian coordinate system and assume length scales are such that the curvature of the field lines are not important.

### III. THE TWO FLUID MODEL AND THE EQUIVALENT DIELECTRIC TENSOR

We first consider the effects of finite  $\beta$  on the linear stability of an infinite inhomogeneous slab of collisionless plasma. The plasma is taken to be of infinite extent with all nonuniformities in the equilibrium model taken in the  $x$  direction. Figure 2 shows the equilibrium physical situation. We consider a nonuniform density and a nonuniform magnetic field along the  $x$ -axis in the equilibrium model. The presence of these nonuniformities leads to a diamagnetic drift of electrons and ions in the  $y$  direction. Additionally we consider an equilibrium flow in the  $z$ -direction with equal ion and electron velocities. This flow is assumed to have a velocity profile which is a function of the  $x$ -coordinate. All gradients are assumed to be weak.

To investigate the stability of the nonuniform plasma slab we will use the equivalent dielectric tensor approach (63, p. 9). The formulation is based using Maxwell's equations to form a "dielectric tensor" for the plasma. In rationalized MKS unit we have

$$\nabla \cdot \vec{D} = \rho_c \quad (3.1a)$$

$$\nabla \cdot \vec{B} = 0 \quad (3.1b)$$

$$\nabla \times \vec{E} = -\frac{\partial \vec{B}}{\partial t} \quad (3.1c)$$

$$\nabla \times \vec{H} = \vec{J} + \frac{\partial \vec{D}}{\partial t} \quad (3.1d)$$

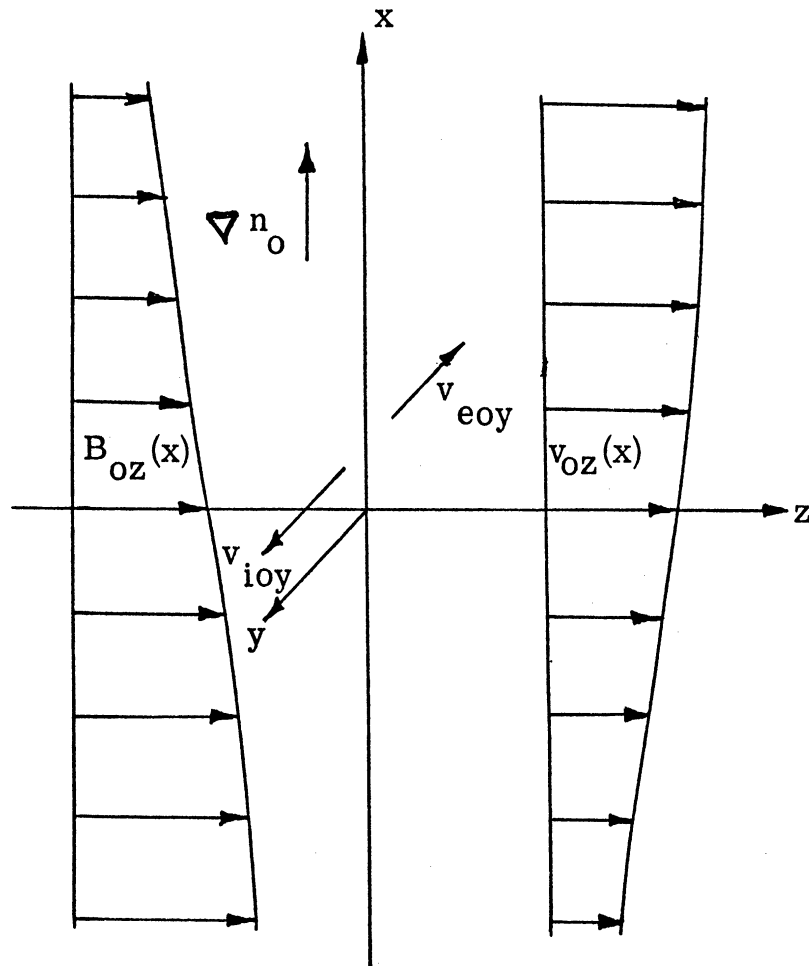


Figure 2. Inhomogeneous Slab Shear Layer Model

The constitutive relations are

$$\vec{B} = \mu_0 \vec{H} \quad (3.2a)$$

$$\vec{D} = \epsilon_0 \vec{E} \quad (3.2b)$$

where  $\mu_0$  and  $\epsilon_0$  are the permeability and dielectric constants for free space. In the above  $\vec{J}$ , the current density, and  $\rho_c$ , the charge density are determined by the plasma. Formally

$$\rho_c = e(n_i - n_e) \quad (3.3a)$$

$$\vec{J} = e(n_i \vec{v}_i - n_e \vec{v}_e) \quad (3.3b)$$

where  $n_i$ ,  $v_i$  and  $n_e$ ,  $v_e$  are the number density and fluid velocity of ions and electrons respectively. These can be obtained from the species fluid equations as will be done here, or from kinetic theory, by taking velocity moments of the distribution function.

Using Eq. (3.2a) and (3.2b) in Eq. (3.1c) and (3.1d) we obtain a single equation in  $\vec{E}$  and  $\vec{J}$

$$\nabla \times (\nabla \times \vec{E}) = -\mu_0 \frac{\partial \vec{J}}{\partial t} - \frac{1}{c^2} \frac{\partial^2 \vec{E}}{\partial t^2}. \quad (3.4)$$

In solving either the fluid equations or the Vlasov equation (since the plasma is collisionless),  $\vec{J}$  will be determined as a function of the electric field  $\vec{E}$ . Thus formally we now define the conductivity tensor  $\vec{\sigma}$  as follows:

$$\vec{J} = \vec{\sigma} \cdot \vec{E}, \quad (3.5)$$

Using the conductivity tensor we rewrite Eq. (2.4)

$$\nabla \times (\nabla \times \vec{E}) + \frac{1}{c^2} \frac{\partial^2 \vec{E}}{\partial t^2} + \mu_0 \vec{\sigma} \cdot \vec{E} = 0. \quad (3.6)$$

This can be written in the form

$$\vec{K} \cdot \vec{E} = 0 \quad (3.7)$$

where  $\vec{K}$  is the equivalent dielectric tensor of the plasma. The operator  $\vec{K}$  is a second order differential operator.

$$\vec{K} = \nabla \times [\nabla \times ( )] + \frac{1}{c^2} \frac{\partial^2 ( )}{\partial t^2} + \mu_0 \vec{\sigma} \cdot ( )$$

For low frequency hydromagnetic waves, which we will be considering, the above relation can be simplified by neglecting the effects of the high frequency displacement current contributions (45, p. 194). This results in neglecting the  $\partial^2 \vec{E} / \partial t^2$  term in  $\vec{K}$  which can now be written

$$\vec{K} = \nabla \times [\nabla \times ( )] + \mu_0 \vec{\sigma} \cdot ( ), \quad (3.8)$$

In the linearization procedure which follows,  $\vec{K}$  will be reduced to an algebraic operator. From this form, the dispersion relation can be obtained for waves propagating in the plasma.

The plasma model is described by the collisionless two fluid hydromagnetic equations for ions and electrons. We also assume

(i) an isotropic pressure tensor for each species, (ii) the plasma is at all times quasineutral ( $n_i \approx n_e = n$ ), and (iii) that the effects of the finite ion Larmor radius are negligible ( $a_i^2/\ell^2 \ll 1$ ,  $\omega^2/\Omega_i^2 \ll 1$ ; where  $\ell$  is the smallest characteristic length and  $\omega$  is the lowest frequency).

The two fluid equations given below can be derived directly from the Vlasov equation by the velocity moment method (45, p. 196).

Bowers and Haines (8) have obtained these equations for higher order in the finite Larmor radius terms at finite  $\beta$  for an isotropic pressure tensor. Macmahon (41) has obtained the same type of equations for a non-isotropic kinetic pressure tensor of the CGL form.

With the above assumptions the ion equations of motion can be written:

Continuity:

$$\frac{\partial n}{\partial t} + \nabla \cdot n \vec{v}_\perp = 0 \quad (3.9)$$

Momentum:

$$\frac{\partial \vec{v}_\perp}{\partial t} + \vec{v}_\perp \cdot \nabla \vec{v}_\perp = -\nabla p_i + en(\vec{E} + \vec{v}_\perp \times \vec{B}) \quad (3.10)$$

Gas Law:

$$p_\perp = n k T_\perp \quad (3.11a)$$

where with  $k$  being Boltzmann's constant

$$T_\perp = k T_i. \quad (3.11b)$$

These equations are closed by a pressure density relation as a simplified energy equation

$$d p_{\perp} = v_{\perp}^2 d \rho_{\perp} \quad (3.12a)$$

where

$$v_{\perp}^2 = \frac{T_{\perp}}{M} \quad \text{for isothermal cases} \quad (3.12b)$$

$$= \gamma \frac{T_{\perp}}{M} \quad \text{for adiabatic cases} \quad (3.12c)$$

$$\rho_{\perp} = n M. \quad (3.13)$$

The above assumptions for the equation of state apply to either problems where state changes are isothermal or adiabatic. In the derivation from the moment expansion of the Vlasov equation they are equivalent to considering a zero heat flux vector (8, 41).

For the electron equations, we introduce one further assumption. Here we assume that the electrons, because of their small mass, remain in equilibrium with the fields. For the stability problem, this implies that the electron thermal velocity is much larger than the phase velocity of the wave produced by the perturbation. Hence the inertia terms in the equation of motion for the electrons may be neglected.

Continuity:

$$\frac{\partial n}{\partial t} + \nabla \cdot n \vec{v}_e = 0 \quad (3.14)$$

Momentum:

$$0 = -\nabla p_e - en(\vec{E} + \vec{v}_e \times \vec{B}) \quad (3.15)$$

Gas Law:

$$p_e = n T_e \quad (3.16)$$

Pressure-Density Relation:

$$d p_e = v_e^2 d \rho_e \quad (3.17a)$$

where again

$$v_e^2 = \frac{T_e}{m} \quad \text{isothermal case} \quad (3.17b)$$

$$= \gamma \frac{T_e}{m} \quad \text{adiabatic case} \quad (3.17c)$$

$$\rho_e = n m \quad (3.18)$$

For the equilibrium configuration assumed previously, Fig. 2, the above set of equations is satisfied exactly with the diamagnetic drifts given by



$$V_{i0y} = \eta \frac{U_a^2}{\Omega_i} - \frac{e}{M} \frac{E_{0x}}{\Omega_i} \quad (3.19a)$$

$$V_{e0y} = -\eta \frac{U_a^2}{\Omega_i} - \frac{e}{M} \frac{E_{0x}}{\Omega_i} \quad (3.19b)$$

where

$$\eta = \frac{1}{n_0} \frac{dn_0}{dx} \quad (3.20)$$

$$E_{0x} = \text{constant (from Poisson's equation)} \quad (3.21)$$

$$U_a^2 = \frac{m}{M} U_e^2 \quad (3.22)$$

$U_a$  is the ion acoustic speed. The above drift velocities were obtained from the x-component of the equilibrium ion and electron momentum equations respectively.

This drift gives rise to a current in the y-direction for the equilibrium model. From Maxwell's curl equation, Eq. (3.1d), we obtain the "standard" hydromagnetic total pressure relation for the equilibrium configuration

$$\frac{d}{dx} \left( p_{i0} + p_{e0} + \frac{B_0^2}{2\mu_0} \right) = 0. \quad (3.23)$$

The total pressure is constant throughout the layer.

It should be noted here that the equilibrium magnetic field is related to the equilibrium density gradient. In the cases considered here

Isothermal case:

$$\kappa_B = \frac{1}{B_0} \frac{dB_0}{dx} = -\frac{\beta}{2} \eta \quad (3.24a)$$

Adiabatic case:

$$\kappa_B = \frac{1}{B_0} \frac{dB_0}{dx} = -\tilde{\gamma} \frac{\beta}{2} \eta. \quad (3.24b)$$

For  $\beta \ll 1$  it was possible to neglect variations of  $B_0$  with  $x$ .

As can be seen from above, as  $\beta$  increases the variation of the equilibrium field with  $x$  must be included.

At this point we will introduce one further assumption. We will consider a situation with "conducting end plates" such that the equilibrium electric field is shorted. We will therefore take

$$\bar{E}_{0x} = 0.$$

For the magnetopause problem the "conducting end plates are provided by the ionosphere. The drift equations now become

$$\begin{aligned} v_{i0y} &= \eta \frac{U_i^2}{\Omega_i} \\ v_{e0y} &= -\eta \frac{U_a^2}{\Omega_i}. \end{aligned} \quad (3.25)$$

To investigate wave propagation in the slab, we linearize the above equations.

$$\begin{aligned} n &= n_0 + n_1 \\ \vec{V}_i &= \vec{V}_{i0} + \vec{V}_{i1} \\ \vec{V}_e &= \vec{V}_{e0} + \vec{V}_{e1} \\ \vec{E} &= \vec{E}_1 \\ \vec{B} &= \vec{B}_0 + \vec{b} \end{aligned}$$

where the variables with subscript 1 are small such that products of perturbed quantities can be neglected. The perturbations are taken to be of the form:

$$f_1(x, y, z, t) = f_1(x) \exp[-i(\kappa_y y + \kappa_z z - \omega t)] \quad (3.26)$$

Substituting into the two fluid equations and Maxwell's equations and after some algebraic manipulation we obtain

Ion Continuity Equation:

$$\begin{aligned} i\omega n_1 v = & \kappa_y V_{iy1} + \kappa_z V_{iz1} \\ & + \frac{dV_{ix1}}{dx} + \eta V_{ix1} \end{aligned} \quad (3.27a)$$

where

$$\omega_{\lambda} = \omega - \kappa_y V_{\lambda 0y} - \kappa_z V_{\lambda 0z} \quad (3.27b)$$

$$\nu = \frac{n_1}{n_0} \quad (3.27c)$$

X-Component Ion Momentum Equation:

$$\begin{aligned} -\lambda \omega_{\lambda} V_{\lambda x1} - \Omega_{\lambda} V_{\lambda y1} &= -U_{\lambda}^2 \frac{d\nu}{dx} + \frac{e \omega_{\lambda}}{M \omega} E_{1x} \\ &- \lambda \frac{e}{M \omega} \left[ V_{\lambda 0y} \frac{dE_{1y}}{dx} + V_{\lambda 0z} \frac{dE_{1z}}{dx} \right] \end{aligned} \quad (3.28a)$$

Y-Component Ion Momentum Equation:

$$\begin{aligned} -\lambda \omega_{\lambda} V_{\lambda z1} + \Omega_{\lambda} \left( 1 + \frac{1}{\Omega_{\lambda}} \frac{dV_{\lambda 0y}}{dx} \right) V_{\lambda x1} &= -\lambda \kappa_y U_{\lambda}^2 \nu \\ &+ \frac{e}{M} \frac{(\omega - \kappa_z V_{\lambda 0z})}{\omega} E_{1y} + \frac{e}{M} \frac{\kappa_z V_{\lambda 0z}}{\omega} E_{1z} \end{aligned} \quad (3.28b)$$

Z-Component Ion Momentum Equation:

$$\begin{aligned} -\lambda \omega_{\lambda} V_{\lambda z1} + \frac{dV_{\lambda 0z}}{dx} V_{\lambda x1} &= -\lambda \kappa_z U_{\lambda}^2 \nu \\ &+ \frac{e}{M} \frac{\kappa_z V_{\lambda 0y}}{\omega} E_{1y} + \frac{e}{M} \frac{(\omega - \kappa_y V_{\lambda 0y})}{\omega} E_{1z} \end{aligned} \quad (3.28c)$$

Electron Continuity Equation:

$$+ \lambda \omega_e v = i \kappa_y v_{ey1} + i \kappa_z v_{ez1} + \frac{d}{dx} v_{ex1} + \eta v_{ex1} \quad (3.29a)$$

where

$$\omega_e = \omega - \kappa_y v_{ey0} - \kappa_z v_{ez0} \quad (3.29b)$$

X-Component Electron Momentum Equation:

$$\begin{aligned} 0 = & -v_a^2 \frac{dv}{dx} - \Omega_e v_{ey1} - \frac{e}{M} \frac{\omega_e}{\omega} E_{1x} \\ & + i \frac{e}{M} \frac{v_{ey0}}{\omega} \frac{dE_{1y}}{dx} + i \frac{e}{M} \frac{v_{ez0}}{\omega} \frac{dE_{1z}}{dx} \end{aligned} \quad (3.30a)$$

Y-Component Electron Momentum Equation:

$$\begin{aligned} 0 = & -\lambda \kappa_y v_a^2 v + \Omega_e v_{ex1} - \frac{e}{M} \frac{(\omega - \kappa_z v_{ez0})}{\omega} E_{1y} \\ & - \frac{e}{M} \kappa_y \frac{v_{ez0}}{\omega} E_{1z} \end{aligned} \quad (3.30b)$$

Z-Component Electron Momentum Equation:

$$\begin{aligned} 0 = & -\lambda \kappa_z v_a^2 v - \frac{e}{M} \kappa_z \frac{v_{ey0}}{\omega} E_{1y} \\ & - \frac{e}{M} \frac{(\omega - \kappa_y v_{ey0})}{\omega} E_{1z}. \end{aligned} \quad (3.30c)$$

For the normal mode expansion given above the dielectric equation

(3.8) becomes

$$\nabla \times (\nabla \times \vec{E}_1) - \lambda \omega n_0 \mu_0 e [\vec{v}_{i1} - \vec{v}_{e1} + \nu (\vec{v}_{i0y} - \vec{v}_{e0y})] = 0 \quad (3.31)$$

The species momentum equations and the electron continuity equation can be solved to give the perturbed number density and species velocities as a function of the perturbed electric field  $\vec{E}_1$ . This leads to the dielectric tensor as indicated earlier. Formally we thus obtain

$$\vec{K} \cdot \vec{E}_1 = 0$$

as indicated earlier. The normal mode expansion, Eq. (3.26), has reduced  $\vec{K}$  to a second order differential operator.

Before writing  $\vec{K}$  explicitly, the dielectric tensor will be reduced to an algebraic form. For weak gradients this reduction is customarily done by assuming the perturbed electric field to be a very weak function of the  $x$ -coordinate. Thus although the equilibrium plasma properties vary with the  $x$ -coordinate, the perturbations of the electric field is taken to be independent of  $x$ . In this case the equilibrium properties which occur in the resulting dispersion relation are evaluated at a local position  $x = x^*$ . This position is usually taken to be

the position of maximum gradient. Under this "local approximation" (35) the differential dielectric tensor is reduced to an algebraic form with the perturbed electric field  $\vec{E}$ , independent of the x coordinate.

The reduction begins by solving the z-momentum equation, Eq. (3.30c) for  $\nu$ .

$$\nu = \frac{\lambda e}{\omega M \kappa_z U_a^2} \left[ \kappa_z v_{e0y} \vec{E}_y + (\omega - \kappa_y v_{e0y}) E_{1z} \right] \quad (3.32)$$

with this value of  $\nu$  we can solve Eq. (3.30a) and (3.30b) for  $v_{ey1}$  and  $v_{ex1}$  respectively. Under the above assumptions we obtain

$$v_{ex1} = \frac{e W_e}{M \omega \Omega_i} \left( E_{1y} - \frac{\kappa_y}{\kappa_z} E_{1z} \right) \quad (3.33a)$$

$$v_{ey1} = -\frac{e W_e}{M \omega \Omega_i} E_{1x} - \frac{\lambda e}{M \omega \Omega_i} \frac{d v_{e0y}}{dx} E_{1y} + \frac{\lambda e}{M \omega \Omega_i} \frac{\kappa_y}{\kappa_z} E_{1z}. \quad (3.33b)$$

The z-component of the electron velocity is obtained by substituting the above in the electron continuity equation, Eq. (3.29a). This yields

$$v_{ez1} = \frac{e W_e}{M \omega \Omega_i} \frac{\kappa_y}{\kappa_z} E_x - \frac{\lambda e}{M \omega \Omega_i} E_{1y} \left( W_e \frac{\kappa_z}{\kappa_z} + \frac{d v_{e0z}}{dx} \right) + \frac{\lambda e}{M \omega \kappa_z U_a^2} \left[ W_e (\omega + \kappa_z \frac{\kappa_y}{\Omega_i} U_a^2) + \kappa_y \frac{\kappa_z}{\Omega_i} U_a^2 \frac{d v_{e0z}}{dx} \right]. \quad (3.33c)$$

Using the value of  $\nu$  from above we solve Eq. (3.28a) and (3.28b), the x-component and y-component of the ion momentum equations,

simultaneously for the x-component and y-component of the perturbed ion velocity. Making the low frequency assumption

$$\frac{\omega^2}{\Omega_i^2} \ll 1$$

we obtain

$$\begin{aligned} v_{ix1} = & -\frac{i e \omega^2}{M \omega \Omega_i^2} \left(1 + \frac{1}{\Omega_i} \frac{d v_{iy0}}{dx}\right) \frac{\bar{E}_{ix}}{\Omega_i} + \frac{e \omega}{M \omega \Omega_i} E_{iy} \\ & + \frac{i e}{M \omega} \frac{\kappa_y}{\kappa_z} \frac{E_{iz}}{\Omega_i} \frac{1}{\left(1 + \frac{1}{\Omega_i} \frac{d v_{iy0}}{dx}\right)} \left[ \frac{\omega \omega^2}{\omega_a^2} \right. \\ & \left. + \kappa_y v_{iy0} + \kappa_z v_{iz} - \frac{1}{\Omega_i} \frac{d v_{iy0}}{dx} \omega \right] \end{aligned} \quad (3.34a)$$

$$\begin{aligned} v_{iy1} = & -\frac{e \omega}{M \omega \Omega_i} E_{ix} - \frac{i e}{M \omega \Omega_i^2} \left(1 + \frac{1}{\Omega_i} \frac{d v_{iy0}}{dx}\right) \frac{E_{iy}}{\Omega_i} \left[ \omega^2 \right. \\ & \left. + \Omega_i \frac{d v_{iy0}}{dx} \left(1 + \frac{1}{\Omega_i} \frac{d v_{iy0}}{dx}\right) \right] - \frac{i e}{M \omega} \frac{\kappa_y}{\kappa_z} \frac{E_{iz}}{\Omega_i^2} \\ & \cdot \frac{1}{\left(1 + \frac{1}{\Omega_i} \frac{d v_{iy0}}{dx}\right)} \left[ \frac{\omega^2}{\omega_a^2} \left( \omega^2 + \kappa_y v_{iy0} + \kappa_z v_{iz} \right) - \Omega_i \frac{d v_{iy0}}{dx} \left(1 + \frac{1}{\Omega_i} \frac{d v_{iy0}}{dx}\right) \right] \end{aligned} \quad (3.34b)$$

The z-component of the ion velocity is obtained by substituting for  $v_{ix1}$  in the z-component of the ion momentum equation, Eq. (3.28c).

This yields



$$\begin{aligned}
v_{iz1} = & -\frac{e}{M\omega\Omega_i} \frac{dv_{oz}}{dx} \frac{W_i E_{ix}}{\left(1 + \frac{1}{\Omega_i} \frac{dv_{ioy}}{dx}\right)} - \frac{e}{M\omega\Omega_i} \frac{dv_{oz}}{dx} E_{iy} \\
& + \frac{e}{M\omega W_i} E_{iz} \left\{ \omega \left[ \frac{U_i^2 + U_e^2}{U_i^2} - \frac{\kappa_y}{\kappa_z} \frac{dv_{oz}}{dx} \frac{(U_i^2/U_e^2)}{\Omega_i \left(1 + \frac{1}{\Omega_i} \frac{dv_{ioy}}{dx}\right)} \right] \right. \\
& \left. - \frac{\kappa_y}{\kappa_z} \frac{dv_{oz}}{dx} \frac{1}{\Omega_i \left(1 + \frac{1}{\Omega_i} \frac{dv_{ioy}}{dx}\right)} \left( \kappa_y v_{ioy} + \kappa_z v_{oz} \right. \right. \\
& \left. \left. - \frac{1}{\Omega_i} \frac{dv_{ioy}}{dx} W_i \right) \right\}. \tag{3.34c}
\end{aligned}$$

Throughout the above analysis we have retained forms containing the  $x$ -derivatives of the ion and electron equilibrium drift velocity.

Two special cases of the above analysis are possible. The first assumes the ion and electron equilibrium drift velocities are constant.

For this case the above derivatives are zero.

$$\frac{dv_{ioy}}{dx} = \frac{dv_{eoy}}{dx} = 0 \tag{3.35}$$

Because of the  $x$ -dependence of the equilibrium magnetic field as well as the  $x$ -dependence of the density the above condition requires

$$\frac{d}{dx} \left( \frac{\eta}{\Omega_i} \right) = 0$$

or

$$\frac{d\eta}{dx} + \frac{\beta}{2} \eta^2 = 0. \tag{3.36}$$

In the above we have used Eq. (3.24a) to express the variation of the equilibrium magnetic field in terms of the variation in the density.

The above equation relates the density and magnetic field variation in the equilibrium model. This gives  $\nu$  independent of  $x$ -variations.

The second special case is the one most often employed in the electrostatic case. This assumes that the equilibrium density variation is exponential. For this case the density variation is given by

$$n_0(x) = N_0 e^{\eta x}$$

This gives

$$\eta = \text{constant.} \quad (3.37)$$

For this case with  $\beta$  not equal to zero it is no longer possible to take the drift velocities constant as was the case for the electrostatic approximation. This can be seen clearly from Eq. (3.36) above. For the exponential density variation case the derivatives of the drift velocities are given for an isothermal plasma by

$$\begin{aligned} \frac{d v_{iy}}{dx} &= -\eta \frac{U_a^2}{\Omega_i} K_B \\ &= \frac{\beta}{2} \eta^2 \frac{U_a^2}{\Omega_i} \end{aligned} \quad (3.38a)$$

$$\frac{d v_{ey}}{dx} = -\frac{\beta}{2} \eta^2 \frac{U_a^2}{\Omega_i}. \quad (3.38b)$$

For the case of constant drift velocities we obtain the following dielectric tensor components:

$$\begin{aligned}
 \underline{K}_{11} &= (\kappa_y^2 + \kappa_z^2) C_A^2 - \bar{W}_\perp^2 \\
 \underline{K}_{12} &= i\eta \kappa_y U_p^2 \\
 \underline{K}_{13} &= -\lambda \frac{\kappa_y}{\kappa_z} \Omega_i \frac{U_p^2}{U_a^2} (\omega - \kappa_y V_{e0y}) \\
 \underline{K}_{21} &= -\lambda \eta \kappa_y U_p^2 \\
 \underline{K}_{22} &= \kappa_z^2 C_A^2 - \eta^2 U_p^2 - \bar{W}_\perp^2 \quad (3.39) \\
 \underline{K}_{23} &= -\kappa_y \kappa_z C_A^2 - \frac{\lambda \kappa_y}{\kappa_z} \left( \frac{U_\perp^2}{U_a^2} \omega + \kappa_y V_{i0y} + \kappa_z V_{0z} \right) \\
 &\quad + \frac{\eta}{\kappa_z} \Omega_i \frac{U_p^2}{U_a^2} (\omega - \kappa_y V_{e0y}) \\
 \underline{K}_{31} &= \lambda \left( \frac{dV_{0z}}{dx} \bar{W}_\perp + \frac{\kappa_y}{\kappa_z} \bar{W}_e \Omega_i \right) \\
 \underline{K}_{32} &= -\kappa_y \kappa_z C_A^2 + \frac{\kappa_z}{\kappa_z} \Omega_i \bar{W}_e \\
 \underline{K}_{33} &= \kappa_y^2 C_A^2 - \frac{\Omega_\perp^2}{\kappa_z^2 U_a^2} \bar{W}_\perp \left\{ \omega \left[ \bar{W}_\perp \bar{W}_e - \kappa_z^2 U_p^2 \left( 1 - \frac{\kappa_y}{\kappa_z} \frac{dV_{0z}}{dx} \right) \right] \right. \\
 &\quad \left. + \bar{W}_\perp \bar{W}_e \kappa_z \kappa_y \frac{U_a^2}{\Omega_i} \right\}
 \end{aligned}$$

where in the above

$$C_A^2 = \frac{B_0^2}{\rho_0 \eta_0 M} \quad (3.40)$$

$$U_p^2 = U_A^2 + U_a^2 \quad (3.41)$$

$C_A$  is the equilibrium Alfvén speed. It should be noted that  $C_A$  is a function of  $x$ .  $\kappa_B$  is related to  $\eta$  by Eq. (3.24). For the case of an exponential density variation the dielectric tensor has the following components:

$$\begin{aligned} \mathbb{K}_{11} &= (\kappa_y^2 + \kappa_z^2) C_A^2 - W_A^2 \\ \mathbb{K}_{12} &= -\lambda \eta \kappa_y U_p^2 \\ \mathbb{K}_{13} &= -\lambda \frac{\kappa_y}{\kappa_z} \Omega_i \left[ \omega \frac{U_p^2}{U_A^2} \left( 1 + \eta \kappa_B \frac{U_A^2}{\Omega_i^2} \right) \right. \\ &\quad \left. + \eta \kappa_y \frac{U_p^2}{\Omega_i^2} + \eta \kappa_B \frac{U_A^2}{\Omega_i^2} W_A^2 \right] \\ \mathbb{K}_{21} &= -\lambda \eta \kappa_y U_p^2 \\ \mathbb{K}_{22} &= \kappa_z^2 C_A^2 - \left( 1 + \kappa_B \eta \frac{U_A^2}{\Omega_i^2} \right) W_A^2 \\ &\quad - \eta U_p^2 (\eta - \kappa_B) \end{aligned} \quad (3.42)$$

$$\begin{aligned} \mathcal{B}_{23} = & -\kappa_y \kappa_z c_A^2 - \frac{\kappa_y}{\kappa_z} \left[ \left( 1 + \eta \frac{\kappa_0 \bar{U}_a^2}{\Omega_a^2} \right) \bar{\omega}_a \left( \frac{\bar{U}_a^2}{\bar{U}_a^2} \omega \right. \right. \\ & \left. \left. + \kappa_y v_{iy} + \kappa_z v_{oz} \right) + \eta \kappa_0 \bar{U}_a^2 \right] + \frac{\eta}{\kappa_z} \frac{\bar{U}_a^2}{\bar{U}_a^2} \\ & \cdot \frac{\Omega_a}{c_A^2} (\omega - \kappa_y v_{ey}) \end{aligned}$$

$$\mathcal{B}_{31} = \omega \left[ \frac{dv_{oz}}{dx} \bar{\omega}_a \left( 1 + \eta \frac{\kappa_0 \bar{U}_a^2}{\Omega_a^2} \right) + \frac{\kappa_y \bar{\omega}_e \Omega_a}{\kappa_z} \right]$$

$$\mathcal{B}_{32} = -\kappa_y \kappa_z c_A^2 + \frac{\kappa_0 \Omega_a \bar{\omega}_e}{\kappa_z}$$

(3.42) cont.

$$\begin{aligned} \mathcal{B}_{33} = & \kappa_y^2 c_A^2 - \frac{\Omega_a^2}{\kappa_z^2 \bar{U}_a^2 \bar{\omega}_a} \left\{ \left[ \bar{\omega}_a \bar{\omega}_e - \kappa_z^2 \bar{U}_a^2 + \kappa_y \kappa_z \bar{U}_a^2 \frac{dv_{oz}}{dx} \right. \right. \\ & \left. \left. \cdot \left( 1 + \frac{\kappa_0 \eta \bar{U}_a^2}{\Omega_a^2} \right) \right] \omega + \bar{\omega}_a \bar{\omega}_e \kappa_y \frac{\kappa_0 \bar{U}_a^2}{\Omega_a} + \kappa_y \kappa_z \bar{U}_a^2 \frac{dv_{oz}}{dx} \bar{\omega}_a \right. \\ & \left. + \kappa_y \kappa_z \bar{U}_a^2 \frac{dv_{oz}}{dx} \left( 1 + \eta \frac{\kappa_0 \bar{U}_a^2}{\Omega_a^2} \right) (\kappa_y v_{iy} + \kappa_z v_{oz} + \eta \frac{\kappa_0 \bar{U}_a^2}{\Omega_a} \bar{\omega}_a) \right\} \end{aligned}$$

With either form of the dielectric tensor Eq. (3.39) or (3.42) it is possible to write out explicitly the equations governing the perturbed electric field in the local region of the disturbance. Formally in matrix notation

$$\begin{bmatrix} \mathcal{B}_{11} & \mathcal{B}_{12} & \mathcal{B}_{13} \\ \mathcal{B}_{21} & \mathcal{B}_{22} & \mathcal{B}_{23} \\ \mathcal{B}_{31} & \mathcal{B}_{32} & \mathcal{B}_{33} \end{bmatrix} \begin{Bmatrix} \bar{E}_{1x} \\ \bar{E}_{1y} \\ \bar{E}_{1z} \end{Bmatrix} = 0. \quad (3.43)$$

#### IV. DISPERSION RELATION AND SOLUTIONS

The dispersion relation for waves propagating in the infinite slab described in Section III is obtained from the solubility conditions for Eq. (3.43). The system of equations described by Eq. (3.43) possesses a nontrivial solution if and only if the determinant of the coefficient matrix  $[K]$  is zero. As can be seen from either the constant drift velocity or the exponential density case, this condition leads to a seventh degree algebraic equation in the frequency. In carrying out the expansion of the determinant it is more convenient to nondimensionalize the elements of the matrix. The following nondimensional frequency is used:

$$\psi = \frac{\omega}{k_2 c_A} \quad (4.1)$$

The formal condition

$$|K| = 0 \quad (4.2)$$

now leads to a seventh degree algebraic equation in the nondimensional frequency  $\psi$ .

$$c_8 \psi^7 + c_7 \psi^6 + c_6 \psi^5 + c_5 \psi^4 + c_4 \psi^3 + c_3 \psi^2 + c_2 \psi + c_1 = 0 \quad (4.3)$$

The coefficients are determined by the dispersion determinant elements. The degree of the determinant requires that numerical

procedures be used to evaluate the roots of Eq. (4.3). With roots taken of the form

$$\omega = \omega_R + i\gamma \quad (4.4)$$

where

$$\omega_R = \text{real part}$$

$$\gamma = \text{imaginary part,}$$

instability will exist for roots with positive imaginary parts.

$$\gamma > 0 \quad \text{for instability}$$

The expansion of the determinant leads to a form of dispersion equation (4.3) with real coefficients. Because of the complexity of the coefficients they will not be written down here. From the theory of equations we know that roots of Eq. (4.3) must be real or complex conjugates.

Before proceeding to evaluate the roots for the finite  $\beta$  case we shall take the electrostatic limit of Eq. (3.39) and (3.42). For this case the perturbed electric field will be taken of the form

$$\vec{E}_1 = -\nabla\phi_1$$

with

$$\phi_1 = \phi_1 \exp\{i(k_y y + k_z z - \omega t)\}$$

and

$$\beta \ll 1.$$

$\phi_1$  is assumed independent of  $x$  as is customary. For this case the equilibrium magnetic field is assumed independent of the  $x$ -coordinate as can be seen from Eq. (3.24). For this case the diamagnetic drift velocities ( $v_{i0y}$ ,  $v_{e0y}$ ) are independent of the  $x$ -coordinate for an exponential density variation. The latter density variation is assumed here. For this case the following relation is obtained from the last equation of the system given by Eq. (3.37).

$$\lambda(\kappa_y \overline{K}_{32} + \kappa_z \overline{K}_{33}) = 0$$

Expanding this equation for

$$\kappa_y^2 a_n^2 \ll 1$$

$$\kappa_z^2 a_n^2 \ll 1$$

$$\eta^2 a_n^2 \ll 1$$

and

$$\beta \ll 1$$

gives

$$W_n^2 + \eta \kappa_y \frac{U_p^2}{\Omega_i} W_n - \kappa_z U_p^2 \left[ \kappa_z - \kappa_y \frac{d v_{0z}}{dx} \right] \frac{1}{\Omega_n} = 0.$$

For an isothermal plasma ( $T_i = T_e$ ) this agrees with D'Angelo's results (14). Solution of the above yields



$$\tau_{\omega} = -\eta \frac{\kappa_y U_{\omega}^2}{\Omega_i} + \frac{1}{2} \left\{ 4\eta^2 \frac{\kappa_y^2 U_{\omega}^4}{\Omega_i^2} + 8\kappa_z^2 U_{\omega}^2 \left( 1 - \frac{\kappa_y}{\kappa_z} \frac{dV_{0z}}{dx} \right) \right\}^{1/2}$$

Instability occurs for

$$\frac{1}{\Omega_i} \frac{dV_{0z}}{dx} > \frac{\kappa_z}{\kappa_y} \left( 1 + \eta^2 \frac{\kappa_y^2 U_{\omega}^2}{2\kappa_z^2 \Omega_i^2} \right) \quad (4.6)$$

in agreement with D'Angelo.

Returning to the finite  $\beta$  case Eq. (4.3) must be solved numerically. Solutions were obtained for both the constant diamagnetic drift velocity and exponential density cases by means of a double precision quotient-difference (QD) algorithm with displacement. This algorithm is a stored subroutine in the IBM scientific subroutine package (SSP) in use with the University of Michigan System 360-67 computer. This subroutine solves for the real and imaginary roots of an nth degree algebraic equation with real coefficients. A complete description of the algorithm, DPRQD, is given in Ref. 30.

Growth rate curves have been obtained for various values of the plasma parameters. These calculations were carried out for an isothermal plasma with equal ion and electron temperatures and  $\beta = 1$ . Since the inconsistency in the zero thickness theory occurs at short wavelengths and since the validity of the local approximation and

neglecting boundary effects is questionable for long wave perturbations, we consider here only short wavelength cases where  $\eta/k_z < 1$  and  $(1/v_o)(d.v_o/dx)/k_z < 1$ . For these cases the length scale of the perturbation is less than the length scale of the nonuniformities. In discussing the results the following nondimensional parameters will be used:

$$\begin{aligned} \Pi &= \frac{\gamma}{k_z c_A} & \Lambda &= \frac{\eta}{k_z} & \Lambda_\sigma &= \frac{\frac{dv_{oz}}{dx}}{k_z v_{oz}} \\ \sigma &= \frac{v_{oz}}{c_A} & \kappa &= \frac{k_y}{k_z} \end{aligned}$$

Solutions were obtained by two procedures. The first of these fixed the density gradient with respect to the ion Larmor radius by fixing  $\epsilon_g = \eta a_i$ .  $\Lambda$ ,  $\Lambda_\sigma$ ,  $\sigma$ , and  $\kappa$  were then varied. For this case changes in  $\Lambda$  show the effects of varying  $k_z$  with  $\eta$  fixed. For fixed  $\Lambda$  changes in  $\Lambda_\sigma$ ,  $\sigma$ , and  $\kappa$  indicate changes in shear, local shear speed, and  $k_y$  respectively. Changing  $\Lambda$  indicates a change in  $k_z$ . Since  $\Lambda_\sigma$  and  $\kappa$  are normalized with respect to  $k_z$  a change in  $\Lambda$  also changes  $\Lambda_\sigma$  and  $\kappa$  for fixed shear and  $k_y$ . The second procedure fixes  $k_z$  by fixing  $\epsilon = k_z a_i$ . For this case a change in  $\Lambda$ ,  $\Lambda_\sigma$ ,  $\sigma$ , and/or  $\kappa$  indicates a change in density gradient, velocity shear, local shear speed, and/or  $k_y$  respectively. Some representative curves are shown in Fig. 3-6.

Figures 3 and 4 show the effect of the velocity shear on the instability. From these it can be seen that the growth rate increases with increasing shear ( $\Lambda_\sigma$ ) and shear flow speed ( $\sigma$ ). Velocity shear thus tends to be destabilizing as could be expected from the hydromagnetic and electrostatic approximation problems. The effects of the density gradient at constant shear conditions can be seen in Fig. 5. The results show the effects of changing the density gradient for a fixed wave number. Here  $k_z$  is fixed by fixing  $\epsilon$ . For this case changes in  $\Lambda$  represent changes in the density gradient. These solutions show that increasing the density gradient leads to a decrease in the growth rate in the  $\Lambda < 1$  region under investigation here. An increasing density gradient thus tends to be stabilizing. This again agrees with the results obtained by D'Angelo for the  $\beta \ll 1$  case. For the  $\Lambda < 1$  case it can be noted from Fig. 4 that the difference in assuming constant diamagnetic drift velocities or an exponential density variation are very small. The results become larger with increasing  $\Lambda$ , however.

It can also be seen from the figures that the growth rate is finite for all cases calculated. If the gradients are fixed ( $\Lambda$ ,  $\Lambda_\sigma$ , and  $\sigma$  constants) and  $k_y$  and  $k_z$  varied it can also be seen that the growth rate decreases as  $k_y$  and/or  $k_z$  become large. In this respect the short wavelength disturbances are stabilized; the growth rate is decreased

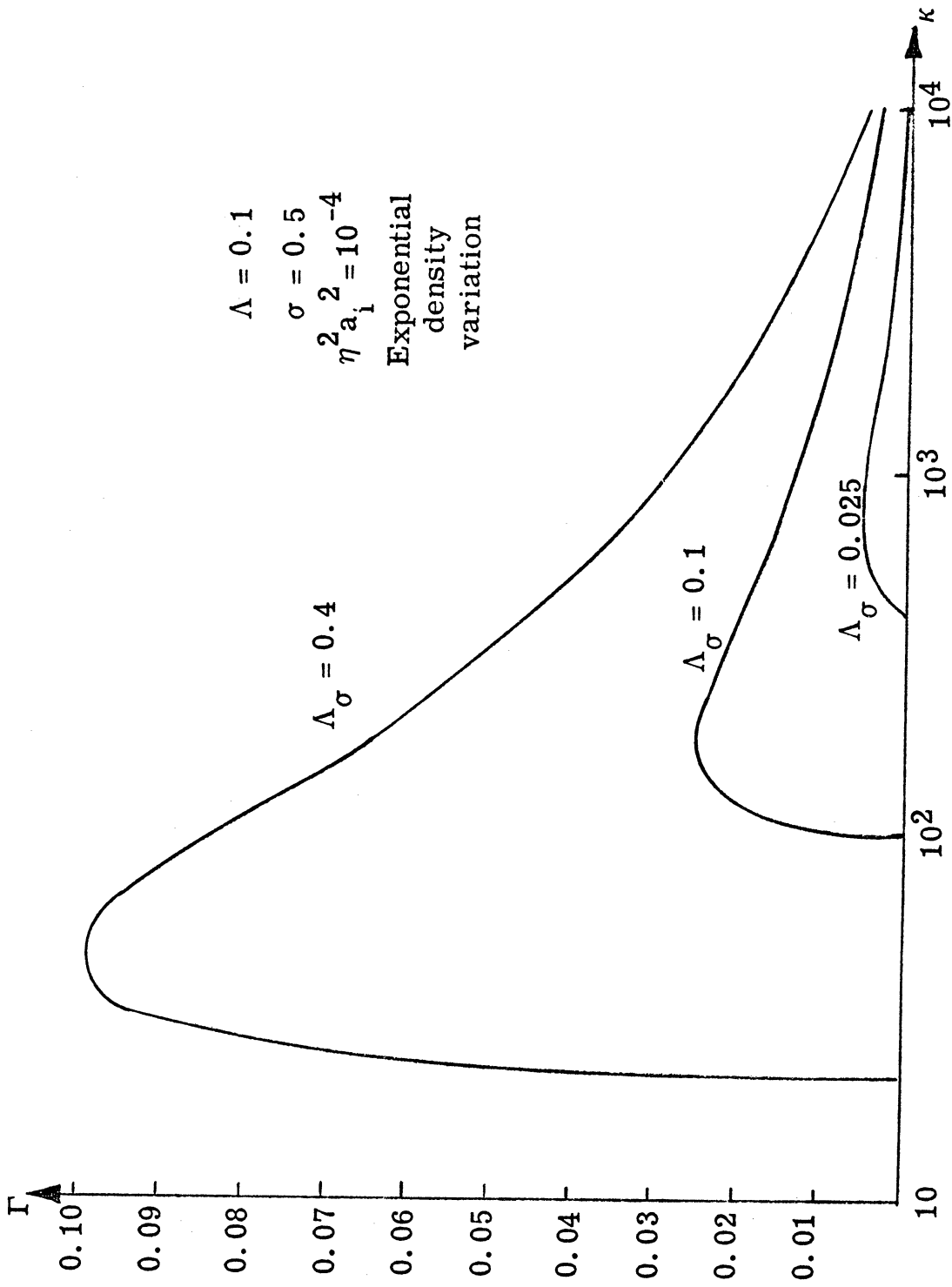


Figure 3. Growth Rate vs Wave Number Ratio. Effects of Velocity Shear

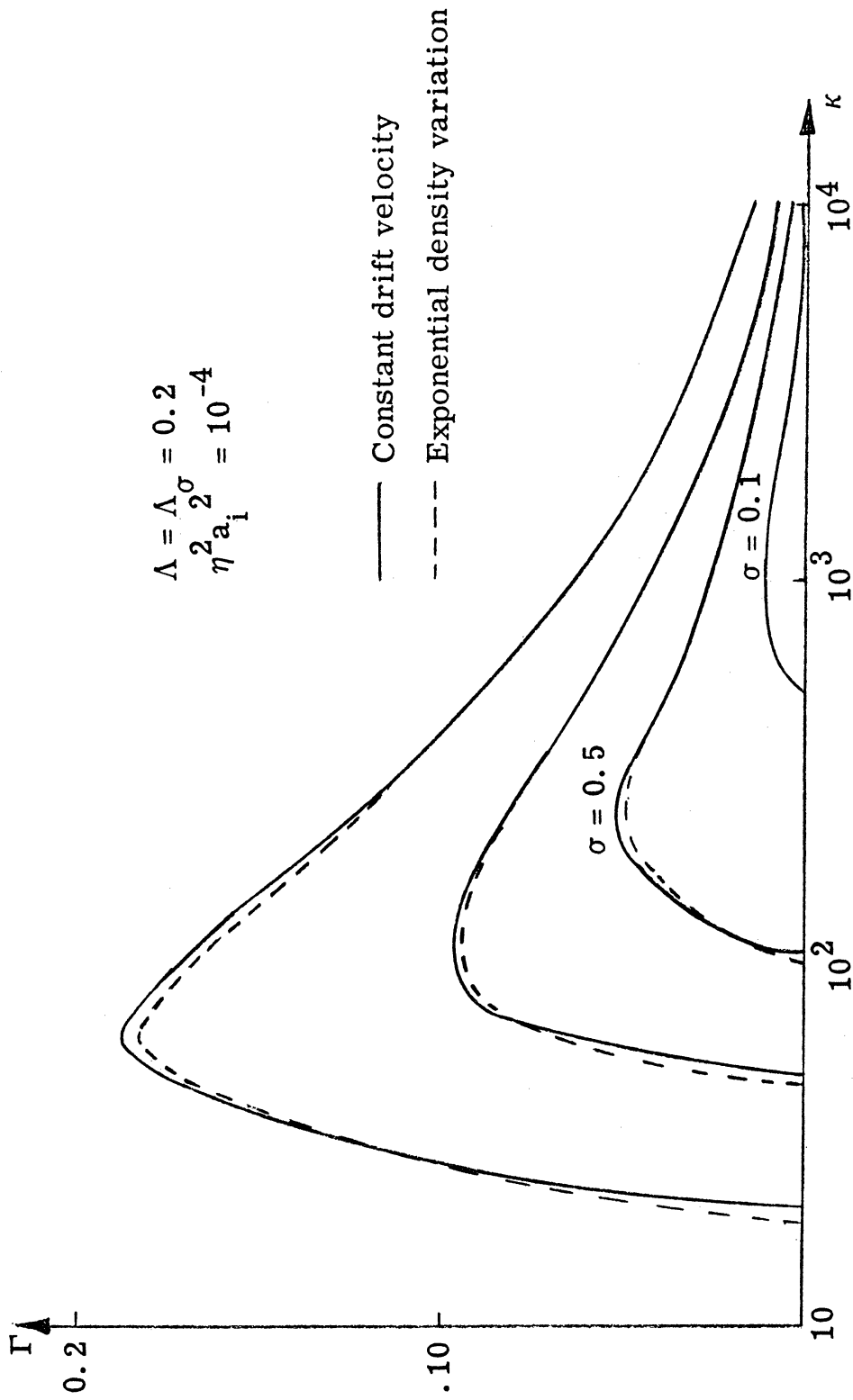


Figure 4. Growth Rate vs Wave Number Ratio. Effects of Local Shear Flow Speed

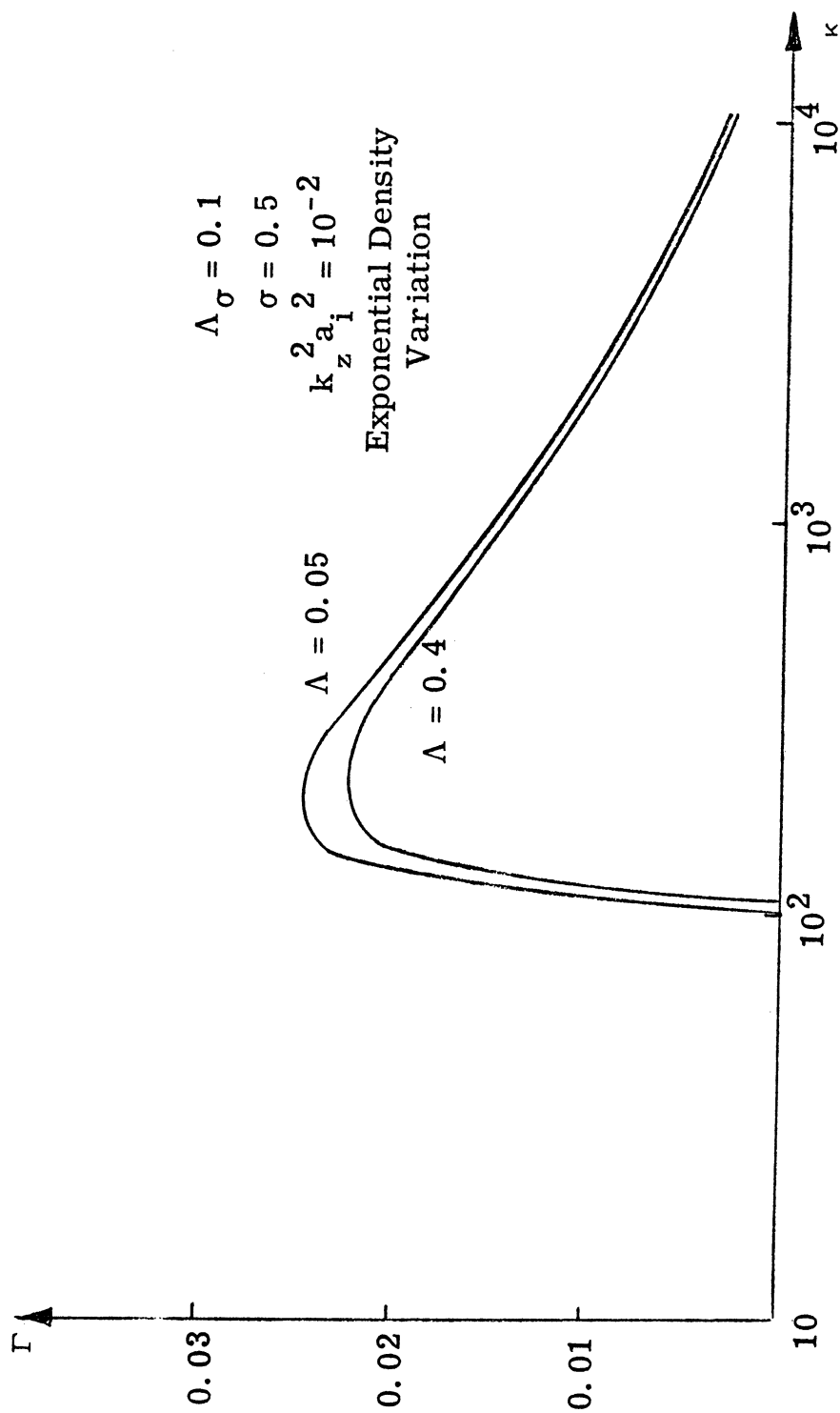


Figure 5. Growth Rate vs Wave Number Ratio. Effects of Density Gradients

as the wavelength becomes small. Because of the complexity of the dispersion relation, Eq. (4.4) it is not possible to obtain analytic expressions for the magnitude of the shear necessary for instability.

In summary for the local approximation with weak gradients and  $\Lambda < 1$  a hydromagnetic velocity shear instability does occur in a  $\beta = 1$  isothermal infinite inhomogeneous plasma slab. The growth rate increases with increasing shear and/or local shear flow velocity while an increasing density gradient at fixed shear conditions decreases the growth rate. In the  $\Lambda < 1$  region the results are nearly identical for either the constant diamagnetic drift velocity or exponential density distribution case. In all cases the growth rate remains finite for all wave numbers and decreases with increasing wave number. Two limits exist to the general extension of the above results to all wave numbers. The first limit is the very short wavelength limit imposed by the finite size of the mean ion Larmor radius. To properly include these effects, one considers the kinetic theory formulation of this problem. The second limit concerns the applicability of the local assumption at the long wavelength limit. As the density gradient and/or the velocity shear increases ( $\Lambda > 1$  and/or  $\Lambda_{\sigma} > 1$ ) the theory of weak gradients and an infinite plasma slab become less valid. For these cases boundary effects must be included. This leads to the study of the hydromagnetic stability of a velocity shear layer of finite thickness.

## V. SINGLE FLUID EQUATIONS AND FINITE THICKNESS MODEL

To investigate the effects of a finite shear layer on the hydromagnetic Kelvin-Helmholtz instability, we shall employ the single fluid hydromagnetic equations as used in the zero thickness models.

These equations can be obtained from the two fluid model considered in the previous section as outlined by Tannenbaum (68, p. 138).

As in the preceding sections, we consider the plasma to be collisionless but with an isotropic pressure tensor. The continuity equation is obtained by adding the electron and ion continuity equations.

$$\frac{\partial}{\partial t} (\eta_i M + \eta_e m) + \nabla \cdot (\eta_i M \vec{v}_i + \eta_e m \vec{v}_e) = 0$$

Defining the global density  $\rho$  and velocity of the plasma  $\vec{v}$  as

$$\rho = M\eta_i + m\eta_e \quad (5.1)$$

$$\rho \vec{v} = M\eta_i \vec{v}_i + m\eta_e \vec{v}_e \quad (5.2)$$

we obtain the single fluid continuity equation

$$\frac{\partial \rho}{\partial t} + \nabla \cdot \rho \vec{v} = 0. \quad (5.3)$$

Adding the electron and ion momentum equations and using Eq. (5.1)

and (5.2) we obtain

$$\rho \left[ \frac{\partial \vec{v}}{\partial t} + \vec{v} \cdot \nabla \vec{v} \right] = -\nabla p_e + \vec{j} \times \vec{B}. \quad (5.4)$$



In the above we have employed the quasineutrality assumption made earlier and have denoted

$$\rho = \rho_i + \rho_e \quad (5.5a)$$

$$\vec{J} = e (\eta_i \vec{v}_i - \eta_e \vec{v}_e). \quad (5.5b)$$

If the fluid is considered compressible a pressure density relation is needed. This now becomes

$$d\rho = c_s^2 d\rho \quad (5.6)$$

where  $c_s^2$  is the adiabatic sound speed for the fluid as a whole.

$$c_s^2 = \gamma RT$$

This equation assumes that the percentage change in each species is nearly equal during compression or rarefaction as for a mixture of perfect gases (68, p. 143).

An Ohm's Law is obtained by taking the explicit expressions for  $\vec{v}_i$  and  $\vec{v}_e$  in terms of  $\vec{v}$  and  $\vec{J}$  and substituting into the electron momentum equation. Specifically

$$\rho_e \vec{v}_e = \frac{mM}{(m+M)} \left( \rho \frac{\vec{v}}{M} - \frac{\vec{J}}{e} \right)$$

$$\rho_i \vec{v}_i = \frac{mM}{(m+M)} \left( \rho \frac{\vec{v}}{m} + \frac{\vec{J}}{e} \right).$$

Substituted into the electron momentum equation yields

$$\vec{E} + \vec{v} \times \vec{B} = \frac{1}{e\rho} \left[ M \left( \rho_i \frac{\partial \vec{v}_i}{\partial t} + \vec{v}_i \cdot \nabla \vec{v}_i + \nabla p_i \right) - m \left( \rho_e \frac{\partial \vec{v}_e}{\partial t} + \vec{v}_e \cdot \nabla \vec{v}_e + \nabla p_e \right) \right].$$

Following the usual hydromagnetic assumption, we take the terms on the right hand side of the above equal to zero (68, p. 158). Thus we obtain the standard Ohm's Law form used by the previous authors (40, 61).

$$\vec{E} + \vec{v} \times \vec{B} = 0 \quad (5.7)$$

Equations (5.3), (5.4), (5.6), and (5.7) along with the low frequency Maxwell's equations, Eq. (3.1), complete the hydromagnetic single fluid description of the plasma. The electric field may be eliminated from Eq. (3.1c) and (5.7) to yield a magnetic field transport equation

$$\frac{\partial \vec{B}}{\partial t} + \vec{v} \cdot \nabla \vec{B} = \vec{B} \cdot \nabla \vec{v} + \vec{B} \nabla \cdot \vec{v}. \quad (5.8)$$

The physical model for the finite shear layer investigation is shown in Fig. 6. We consider a shear layer of thickness  $2d$  in the  $y$ - $z$  plane of a cartesian coordinate system. The layer separates two regions of infinitely conducting fluid. In these regions the equilibrium fluid and electromagnetic field properties are constant.

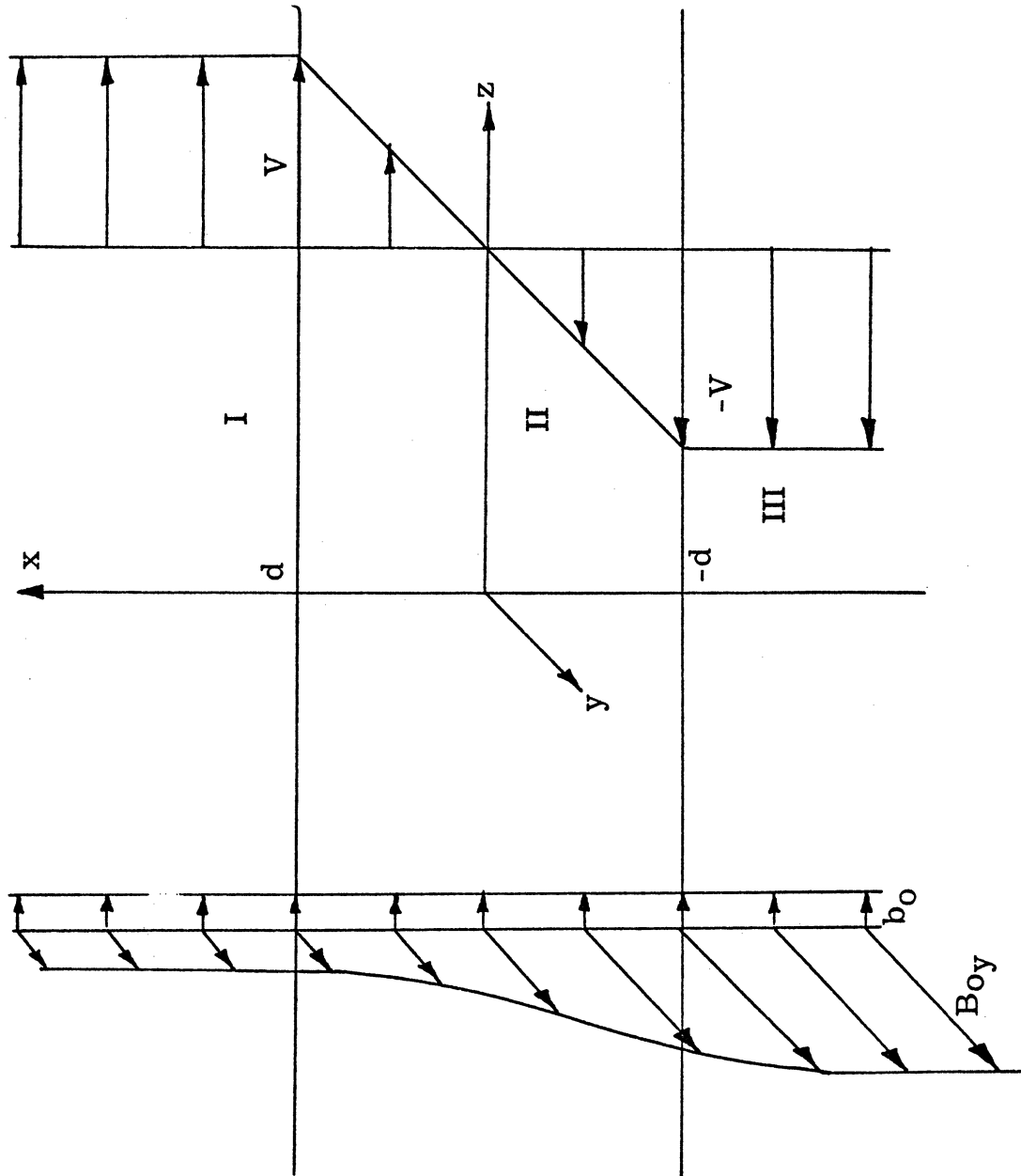


Figure 6. Finite Thickness Shear Layer Model

They vary only inside the layer as shown in Fig. 6. All equilibrium quantities vary only as a function of  $x$ . The equilibrium magnetic field is tangential to the layer. The equilibrium magnetic field is taken of the form

$$\vec{B}_0 = B_{0y}(x) \hat{e}_y + b_0 \hat{e}_z. \quad (5.9)$$

where  $b_0$  is constant. The  $x$ -variation of  $B_{0y}$  is completely arbitrary. The fluid velocity has been transformed in such a way that the constant flow velocities in regions I and III are given by  $v_{0z} = \pm V$  respectively. Its variation through the layer is assumed to be linear.

We now impose a small amplitude disturbance of the normal mode form such that the perturbation quantities vary as  $\exp i(k_y y + k_z z - \omega t)$ . The basic equations above may then be linearized and take the form:

$$+\lambda W \rho_1 = \rho_0 \nabla \cdot \vec{v}_1 + v_{1x} \frac{d\rho_0}{dx} \quad (5.10)$$

$$\begin{aligned} -\lambda W v_{1x} = & -\frac{1}{\rho_0} \frac{d\rho_1}{dx} - \frac{1}{\rho_0 \mu_0} \left[ \frac{d}{dx} (B_{0y} b_y) \right. \\ & \left. + b_0 \left( \frac{db_z}{dx} - \lambda \kappa_z b_x \right) - \lambda \kappa_y B_{0y} b_x \right] \end{aligned} \quad (5.11)$$

$$\begin{aligned} -\lambda W v_{1y} = & -\lambda \kappa_y \frac{\rho_1}{\rho_0} + \frac{b_x}{\rho_0 \mu_0} \frac{dB_{0y}}{dx} \\ & - \lambda \frac{b_0}{\rho_0 \mu_0} (\kappa_y b_z - \kappa_z b_y) \end{aligned} \quad (5.12)$$

$$\begin{aligned}
 -\lambda \bar{W} \kappa_z = V_{ix} \frac{dV_{oz}}{dx} &= -\lambda \kappa_z \frac{\mu_0}{\rho_0} \\
 + \lambda \frac{B_{oy}}{\rho_0 \mu_0} (\kappa_y b_z - \kappa_z b_y) & \quad (5.13)
 \end{aligned}$$

$$-\lambda \bar{W} b_x = \lambda \kappa_z b_0 V_{ix} \quad (5.14)$$

$$\begin{aligned}
 -\lambda \bar{W} b_y + V_{ix} \frac{dB_{oy}}{dx} &= \lambda \kappa_z b_0 V_{iy} \\
 + B_{oy} \nabla \cdot \vec{V}_1 & \quad (5.15)
 \end{aligned}$$

$$\frac{db_x}{dx} + i \kappa_y b_y + i \kappa_z b_z = 0 \quad (5.16)$$

where

$$\bar{W} = \omega - \kappa_z V_{oz}. \quad (5.17)$$

In the equilibrium state the pressure balance across the layer is given by

$$\mu_0 + \frac{B_0^2}{2\mu_0} = \text{constant}. \quad (5.18)$$

In looking at the effects of finite layer thickness we will consider physical conditions such as those encountered at the magnetopause. As mentioned earlier the instability of the magnetopause may occur

in regions where the flow velocity in the magnetosheath is small. This can take place not too far away from the subsolar point. Thus at the point where the instability occurs the flow speed will be very small compared to, say, the local acoustic speed, i. e.  $|V| \ll C_s$  where  $C_s$  is the local speed of sound. These regions of instability as also discussed earlier occur in the low latitude regions near the equatorial plane. The configuration shown in Fig. 6 approximates the flow and magnetic field conditions just off the noon-midnight meridian toward the dusk side near the equatorial plane. The magnetosphere with its relatively large magnetic field is represented by region III. Thus the magnetic field increases from a small value  $B_{01}$  in the magnetosheath (region I) to the larger value  $B_{03}$  in the magnetosphere, with an arbitrary variation taking place inside the magnetopause (region II) which is represented by the finite thickness layer. The equilibrium field may also have a small component parallel to the magnetosheath flow velocity vector. This is represented by the constant  $z$ -component  $b_0$  shown in the figure. Since the flow in the low latitude regions is nearly normal to the magnetic field in the magnetosphere, we assume  $b_0 \ll B_{03}$ . We shall also consider the case of the most unstable mode in the zero thickness formulation. This mode propagates in a direction perpendicular to the magnetic field in the magnetosphere (61). Thus we let

$$\vec{\kappa} \approx \kappa_z \hat{e}_z. \quad (5.19)$$

Since we are considering a physical situation near the subsolar point with  $|V| \ll C_s$  we shall first investigate the incompressible flow limit to the above set of equations and later discuss the effects of compressibility.

## VI. INCOMPRESSIBLE FLOW LIMIT

For incompressible flow the continuity equation, Eq. (5.3)

reduces to

$$\nabla \cdot \vec{v}_1 = 0.$$

In the assumed linearized form this becomes

$$\frac{dV_{1x}}{dx} + \lambda \kappa_y V_{1y} + \lambda \kappa_z V_{1z} = 0.$$

In this case the pressure density relation, Eq. (5.6) is not needed to complete the system of equations. Under the above assumptions, the system of equations now becomes

$$\frac{dV_{1x}}{dx} + \lambda \kappa_z V_{1z} = 0 \quad (6.1)$$

$$\begin{aligned} -\lambda \mathcal{W} V_{1x} = & -\frac{1}{\rho_0} \frac{d\rho_1}{dx} - \frac{1}{\rho_0 M_0} \left[ \frac{d(\beta_{0y} b_y)}{dx} \right. \\ & \left. + b_0 \left( \frac{db_z}{dx} - \lambda \kappa_z b_x \right) \right] \end{aligned} \quad (6.2)$$

$$-\lambda \mathcal{W} V_{1y} = -\frac{b_x}{\rho_0 M_0} \frac{d\beta_{0y}}{dx} + \lambda \frac{\kappa_z b_0}{\rho_0 M_0} b_y \quad (6.3)$$

$$-\lambda \mathcal{W} V_{1z} + V_{1x} \frac{dV_{0z}}{dx} = -\lambda \frac{\kappa_z \rho_1}{\rho_0} - \lambda \frac{\beta_{0y} \kappa_z b_y}{\rho_0 M_0} \quad (6.4)$$

$$-\lambda \mathcal{W} b_x = \lambda \kappa_z b_0 V_{1x} \quad (6.5)$$



$$-\lambda W b_y + v_{1x} \frac{d\beta_{0y}}{dx} = \lambda \kappa_z b_0 v_{1y} \quad (6.6)$$

$$\frac{db_x}{dx} + \lambda \kappa_z b_z = 0. \quad (6.7)$$

To obtain the dispersion relation the above set of equations is reduced to a single ordinary differential equation for the x-component of the perturbation velocity. First Eq. (6.1) and (6.4) are used to express  $p_1/\rho_0$  in terms of  $v_{1x}$  and  $b_y$ :

$$-\frac{\gamma p_1}{\rho_0} = -\lambda \frac{W}{\kappa_z^2} \frac{dv_{1x}}{dx} - \lambda \frac{v_{1x}}{\kappa_z} \frac{dV_{0z}}{dx} + \frac{\beta_0 b_y}{\rho_0 M_0}.$$

This equation is then substituted into Eq. (6.2) and for constant density we obtain

$$-\lambda W v_{1x} = -\frac{d}{dx} \left[ \frac{W}{\kappa_z^2} \frac{dv_{1x}}{dx} + \frac{v_{1x}}{\kappa_z} \frac{dV_{0z}}{dx} \right] - \frac{b_0}{\rho_0 M_0} \left( \frac{db_z}{dx} - \lambda \kappa_z b_x \right).$$

Equation (6.7) is now used to express  $b_z$  in terms of  $b_x$  and then Eq. (6.5) is used to express  $b_x$  in terms of  $v_{1x}$ . Performing this algebraic manipulation yields the following equation for  $v_{1x}$ .

$$\begin{aligned}
& W^2 (W^2 - K_z^2 c_A^2) \frac{d^2 v_{ix}}{dx^2} - 2 K_z^3 c_A^2 \frac{dv_{oz}}{dx} W \frac{dv_{ix}}{dx} \\
& - \left[ K_z W \left( W K_z - \frac{d^2 v_{oz}}{dx^2} \right) (W^2 - K_z^2 c_A^2) + 2 K_z^4 c_A^2 \left( \frac{dv_{oz}}{dx} \right)^2 \right] v_{ix} = 0
\end{aligned} \tag{6.8}$$

where

$$c_A^2 = \frac{b_0^2}{\rho_0 \mu_0}$$

$c_a$  is the Alfvén speed based on the component of the equilibrium magnetic field parallel to the flow velocity. The above equation is valid everywhere for an arbitrary equilibrium shear  $v_{oz}$ , and the boundary conditions are

$$v_{ix} \rightarrow 0 \quad \text{as} \quad x \rightarrow \pm \infty.$$

At the interfaces, the normal displacement of the layer, the normal component of the magnetic field, and the normal stress must be continuous. Assuming a small amplitude displacement of the interface, in line with the linear theory, we can approximately carry out the matching at  $x = \pm d$ .

Outside the layer (regions I and II) the equilibrium flow velocity  $v_{oz}$  is independent of the  $x$ -coordinate. In these regions the solutions to the differential equation, Eq. (6.8), which satisfies the boundary

conditions at  $x = \pm \infty$  are

$$\begin{aligned} v_{1x} &= A_1 \exp(-\kappa_2 x) & \text{for } x > d \\ &= C_3 \exp(\kappa_2 x) & \text{for } x < d \end{aligned} \quad (6.9)$$

where  $A_1$  and  $C_3$  are constants.

Within the transition region (region II) the flow velocity  $v_{oz}$  varies with the  $x$ -coordinate. To treat this case we define a new variable  $\delta$  by

$$\delta = \frac{v_{1x}}{w} \quad (6.10)$$

In terms of  $\delta$  the differential equation (6.9) may be rewritten as

$$\frac{d}{dx} \left[ (W^2 - \kappa_2^2 c_A^2) \frac{d\delta}{dx} \right] - \kappa_2^2 (W^2 - \kappa_2^2 c_A^2) \delta = 0 \quad (6.11)$$

This equation is also valid everywhere with boundary conditions

$$\delta \rightarrow 0 \quad \text{as} \quad x \rightarrow \pm \infty$$

Introducing a further transformation

$$\xi = \kappa_2 x - \Omega \quad (6.12)$$

where

$$\Omega = \frac{\omega d}{V} = \Omega_R + \alpha T$$

we obtain the following differential equation

$$\frac{d}{d\xi} \left[ (\xi^2 - \alpha^2) \frac{d\delta}{d\xi} \right] - (\xi^2 - \alpha^2) \delta = 0 \quad (6.13)$$

where

$$\begin{aligned} \alpha^2 &= \kappa^2 / A^2 \\ \kappa &= \kappa_2 d \\ A^2 &= V^2 / c_A^2. \end{aligned}$$

The edges of the interface are now given by

$$\begin{aligned} x = d &\rightarrow \xi = \xi_1 = \kappa - \Omega \\ x = -d &\rightarrow \xi = \xi_2 = -(\kappa + \Omega). \end{aligned}$$

The solutions in the uniform regions become

$$\begin{aligned} \delta &= A_1 e^{-\xi} && \xi > \xi_1 \\ &= C_3 e^{\xi} && \xi < \xi_2. \end{aligned} \quad (6.14)$$

The dispersion relation is obtained from the condition that the normal displacement, normal component of the magnetic field, and normal component of the stress be continuous at the edges of the shear layer. Continuity of the normal displacement of the interfaces is the same as requiring  $\delta$  to be continuous (11). This is also the result for continuity of the normal component of the magnetic field.

The normal stress condition is obtained by integrating Eq. (6.13), a form of the x-momentum equation, across each interface from  $\xi_{1,2} - \epsilon$  to  $\xi_{1,2} + \epsilon$  and taking the limit as  $\epsilon \rightarrow 0$  ( $\xi_{1,2}$  means the interface edge  $\xi_1$  or  $\xi_2$  respectively). Hence the interface conditions are

$$\begin{aligned}\Delta_{1,2} [\delta] &= 0 \\ \Delta_{1,2} \left[ (\xi^2 - \alpha^2) \frac{d\delta}{d\xi} \right] &= 0,\end{aligned}\tag{6.15}$$

where  $\Delta_{1,2} [ \ ]$  indicates the jump in the quantity inside the square bracket at the interface edge  $\xi_1$  or  $\xi_2$ .

The results for the zero thickness layer are easily obtained from the above. For this case we return to the dimensional form of the problem. In regions I and III we have

$$\begin{aligned}\delta &= A_1 e^{-\kappa_2 x} & x > d \\ &= C_3 e^{\kappa_2 x} & x < -d\end{aligned}$$

$$\Delta_{1,2} [\delta] = 0$$

$$\Delta_{1,2} \left[ \left\{ (\bar{\omega}^2 - \kappa_2^2 \tilde{V}_0^2) - \kappa_2^2 C_A^2 \right\} \frac{d\delta}{dx} \right] = 0.$$

Now taking the limit as  $d \rightarrow 0$  yields the dispersion relation

$$\omega^2 = \kappa_2^2 (C_A^2 - \tilde{V}^2).\tag{6.16}$$

Thus for  $V > c_a$ , or  $1 > 1/A^2$  the interface is unstable. Taking

$$\omega = \omega_R + i \gamma$$

the growth rate of the instability is given by

$$\gamma = k_z V \left( 1 - \frac{c_a^2}{V^2} \right)^{1/2} ; \quad V > c_a. \quad (6.17)$$

This result is the same as that obtained by several previous authors (11). Note that the largest growth rate occurs for disturbances with  $k_z \rightarrow \infty$  (36).

Let us now return to the case where the interface is of finite thickness ( $d \neq 0$ ). Inside the layer Eq. (6.13) is valid. This equation is a spheroidal wave equation with three singular points (47, p. 642). There are two regular singular points at  $\xi = \pm \alpha$  and an irregular singular point at  $\xi = \infty$ . The equation has a general solution in terms of a series expansion in  $\xi$  or an expansion in terms of appropriate functions of  $\xi$ . However, since  $\xi$  contains  $\omega$  the series solution is awkward for the discussion of dispersion relations. Hence it is more convenient to find an approximate solution by means of the WKB procedure. In order to do this we first define a variable  $\zeta$  by

$$d\zeta = \frac{d\xi}{\xi^2 - \alpha^2}.$$

The differential equation (6.13) can then be transformed into the standard form:

$$\frac{d^2 \delta}{dy^2} - [Q(y)]^2 \delta = 0 \quad (6.18)$$

where

$$[Q(y)]^2 = [\xi^2(y) - \alpha^2]^2.$$

For  $Q$  not near zero the asymptotic form of the solution is given by

$$\delta = A_{\pm} \frac{\exp\{\pm \int Q dy\}}{Q^{1/2}}.$$

In terms of the variable  $\xi$  we obtain

$$\delta = \frac{A_+}{(\xi^2 - \alpha^2)^{1/2}} \exp(\frac{\xi}{\alpha}) + \frac{A_-}{(\xi^2 - \alpha^2)^{1/2}} \exp(-\frac{\xi}{\alpha}). \quad (6.19)$$

The WKB validity condition implies that the solution given by Eq.

(6.19) is a valid one provided

$$A^2 \gg 1 \quad \text{for} \quad \kappa \leq O(1) \quad (6.20)$$

and

$$\kappa \gg 1 \quad \text{for} \quad A \leq O(1).$$

It is interesting to note that Eq. (6.19) becomes an exact solution to the differential equation (6.13) for  $A \rightarrow \infty$ . This is the "vanishing parallel magnetic field limit". It corresponds to  $b_0 = 0$ ; this implies

in the magnetopause problem that the magnetic field in the magnetosheath is aligned with the field in the magnetosphere. In this case the results are the same as those obtained by Rayleigh for the hydrodynamic problem. The condition  $A^2 \gg 1$  above indicates that the flow velocity, while small compared to the acoustic velocity, must be large compared to the Alfvén speed based on the parallel magnetic field component  $b_o$ .

Another interesting feature of the incompressible flow case is that the relevant differential equation and its solution are independent of the variation of  $B_{oy}$ . The magnetic field component perpendicular to the direction of the wave normal of the disturbance and the flow velocity does not affect the stability of the shear layer. The same result was obtained in the case of a zero thickness shear layer with a constant perpendicular magnetic field (11).

To obtain the dispersion relation for this case we again use the matching condition at the edges of the interface region, Eq. (6.15). Since for this case  $\xi$  is continuous at the edges the second relation becomes

$$\Delta_{1,2} \left[ \frac{d\delta}{d\xi} \right] = 0. \quad (6.21)$$

For  $A_1$ ,  $C_3$ ,  $A_+$ , and  $A_-$  non-zero we obtain the following dispersion relation:



$$\Omega^4 + \Omega^2 \left\{ \kappa - 2\kappa^2 \left( 1 + \frac{1}{A^2} \right) - \frac{1}{4} [\exp(-4\kappa)] \right\} + \kappa^4 \left( 1 - \frac{1}{A^2} \right)^2 - \kappa^3 \left( 1 - \frac{1}{A^2} \right) + \frac{\kappa^2}{4} [1 - \exp(-4\kappa)] = 0. \quad (6.22)$$

For  $A \rightarrow \infty$  this reduces to the dispersion relation in the hydrodynamic case with no magnetic field.

$$\Omega^2 = \left( 1 - \frac{2\kappa}{4} \right)^2 - \frac{e^{-4\kappa}}{4}$$

Since Eq. (6.22) is a biquadratic equation for  $\Omega$  it is possible in principle to write out explicit solutions for  $\Omega$  by means of the quadratic formula. Formally we can thus write

$$\Omega^2 = \frac{-1}{2} \left\{ \kappa - 2\kappa^2 \left( 1 + \frac{1}{A^2} \right) - \frac{[1 - \exp(-4\kappa)]}{4} \right\} + \frac{1}{2} \left\{ \left[ \kappa - 2\kappa^2 \left( 1 + \frac{1}{A^2} \right) - \frac{1}{4} + \frac{\exp(-4\kappa)}{4} \right]^2 - 4 \left[ \kappa^4 \left( 1 - \frac{1}{A^2} \right)^2 - \kappa^3 \left( 1 - \frac{1}{A^2} \right) + \frac{1}{4} - \frac{\exp(-4\kappa)}{4} \right] \right\}^{1/2}$$

Because of the complexities of the above form for  $\Omega^2$  we have evaluated the roots of Eq. (6.22) numerically. Typical growth rate versus non-dimensional wave number curves are shown in Fig. 7. The

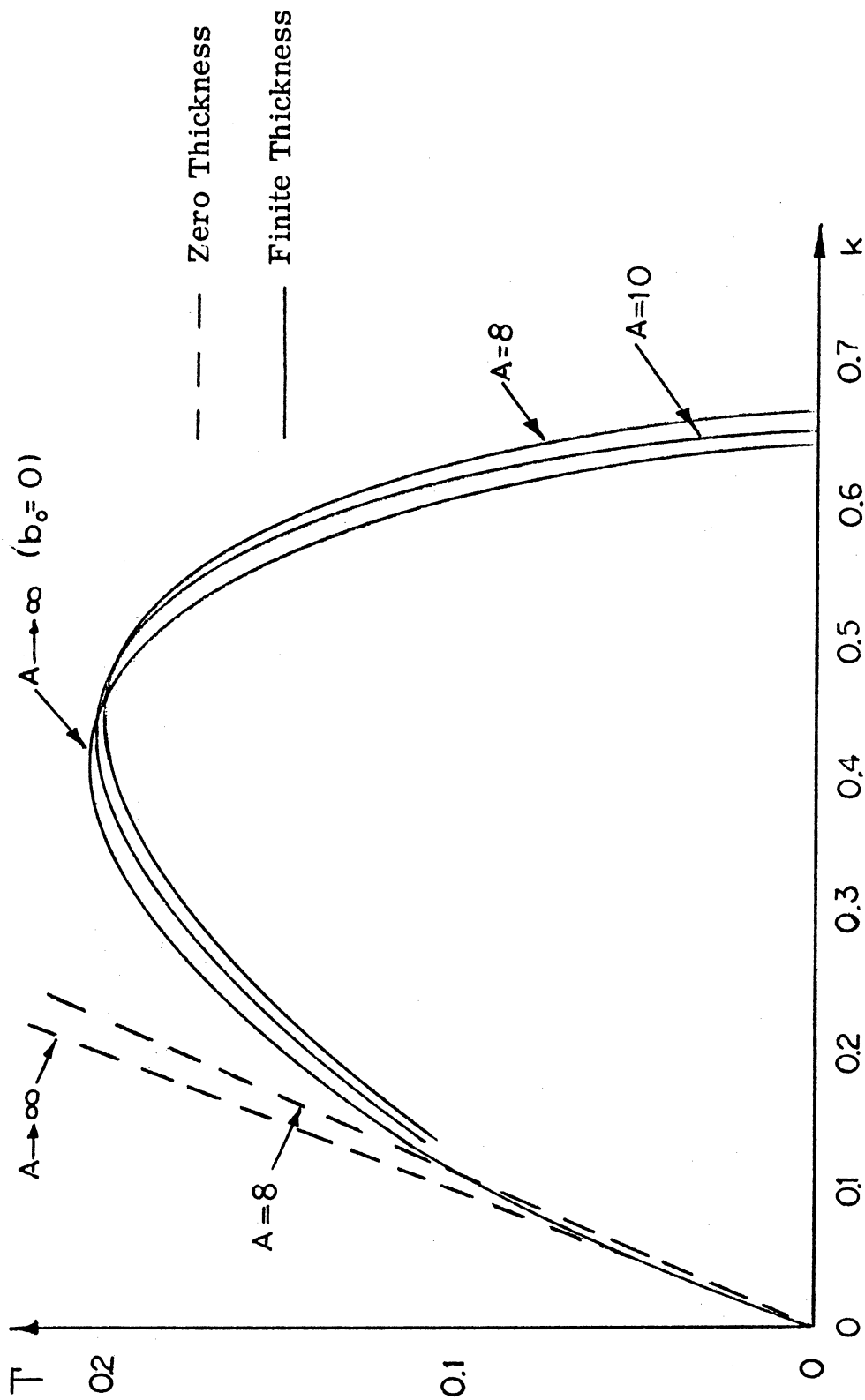


Figure 7. Growth Rate vs Wave Number. Effects of Finite Thickness and Parallel Magnetic Field

$c_a \neq 0$  growth rate curves shown are for relatively large values of the Alfvén Mach number based on the parallel component of the magnetic field. For this case the WKB solution is valid in the  $k \leq O(1)$  region. The well known results for the case of a zero thickness shear layer are also shown for comparison.

These results show the existence of a critical wave number  $k_c$  such that for  $k > k_c$  the growth rate of the disturbance is zero. When we have a non-zero parallel magnetic field  $b_0$  the maximum value of the growth rate of the instability is reduced. Thus for a shear layer of certain thickness the parallel component of the magnetic field in this sense tends to stabilize the flow. There now exists a region of wave numbers from the  $b_0 = 0$   $k_c$  to the  $k_c$  for  $b_0 \neq 0$  for which the flow is now unstable. Since the maximum growth rate determines the physical behavior of the interface, however, the overall effect is a stabilizing one in the sense that the maximum growth rate is lower for  $b_0 \neq 0$ . The exact value for  $k_c$  is given by the  $\Omega = 0$  condition which from Eq. (6.22) is given by the transcendental form:

$$\begin{aligned} k_c^2 \left(1 - \frac{1}{A^2}\right)^2 - k_c \left(1 - \frac{1}{A^2}\right) \\ + \frac{1}{4} [1 - \exp(-4k_c)] = 0. \end{aligned} \quad (6.23)$$

$k_c$  versus  $A$  is plotted in Fig. 8.

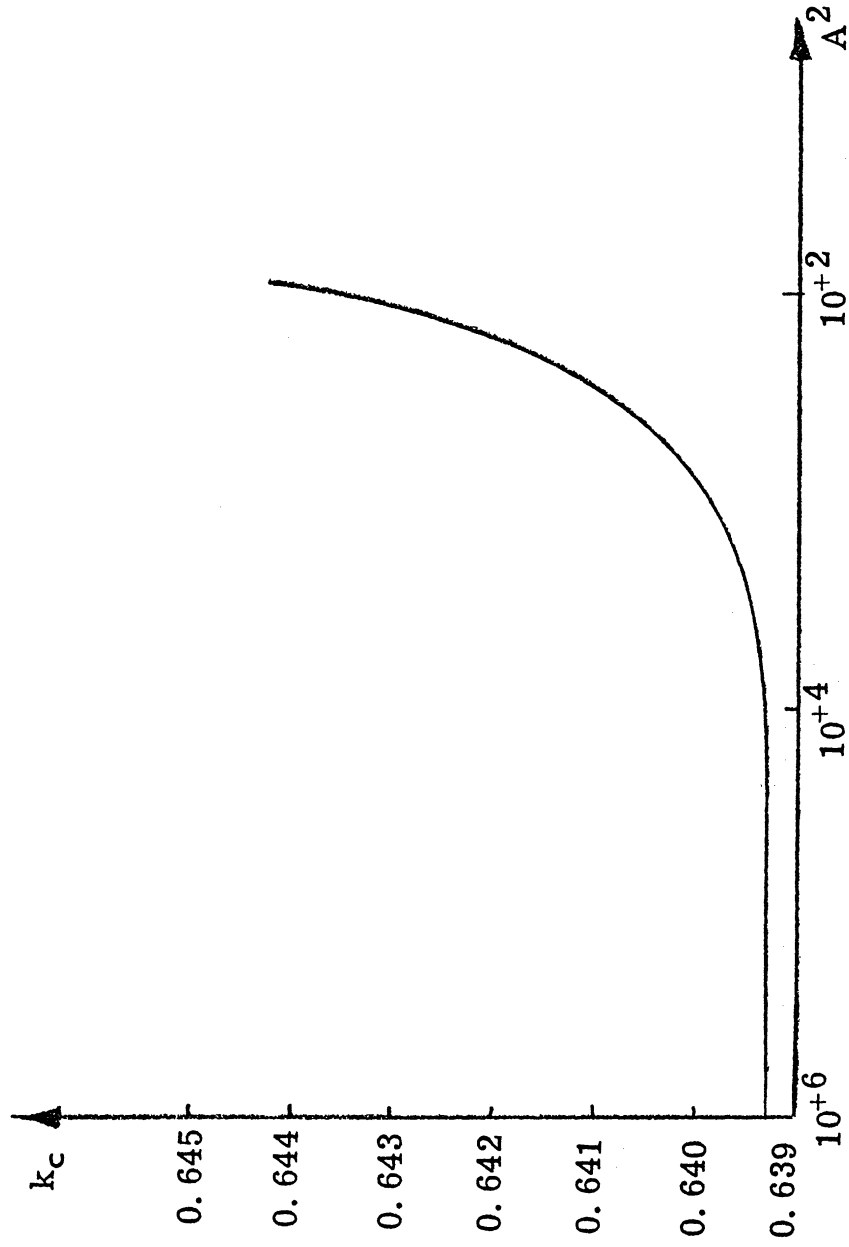


Figure 8. Neutral Stability Wave Number. Effects of Parallel Magnetic Field

For smaller values of  $A$  the WKB approximation breaks down in the  $k < O(1)$  region. In these cases we cannot obtain a quantitative description for the growth rate in the region of the  $\Gamma$ - $k$  plane shown. It is possible to obtain information on the growth rate for large values of  $k$ , however, for all values of  $A$ . For  $k \gg 1$  the WKB approximation remains valid for all  $A$ . Calculations in these regions show  $\Gamma = 0$  for even  $A < 1$ . Quantitatively we can thus say that the growth rate is zero for large values of  $k$  in contrast to the zero thickness theory. Qualitatively we can consider that there exists a  $k_c$  such that the growth rate is zero for all  $k > k_c$  for any value of the parallel field Alfvén Mach number.

In summary, the finite thickness of the shear layer stabilizes it in regard to short wavelength perturbations. With respect to long wavelength disturbances it limits the growth rate to finite values. A parallel magnetic field component  $b_0$  tends to stabilize the layer even further by lowering the maximum growth rate, but it extends the value of the critical wave number somewhat. Two additional special cases of the incompressible flow limit are discussed in the Appendix. The results for these cases are the same as those given above.

## VII. EFFECTS OF COMPRESSIBILITY

In order to study the effects of compressibility we first introduce the following simplifications to our model. The y-component of the magnetic field  $B_{oy}$  will be taken to be constant, while the z-component will be taken equal to zero. The latter assumption leads to the maximum growth rate for the incompressible case. These simplifications do not influence the basic effects of compressibility on the plasma. Since the density is now variable the full form of the continuity equation as given by Eq. (5.3) must be used along with the pressure-density relation given by the adiabatic equation of state, Eq. (5.6). The set of equations under consideration including the assumptions above and parallel propagation reduce to the following:

$$-i\omega\rho_1 + \rho_0\nabla\cdot\vec{v} + v_{ix}\frac{d\rho_0}{dx} = 0 \quad (7.1)$$

$$-i\omega v_{ix} = -\frac{1}{\rho_0}\frac{d\rho_1}{dx} - \frac{B_{oy}}{\rho_0\mu_0}\frac{db_y}{dx} = 0 \quad (7.2)$$

$$-i\omega v_{iy} = 0 \quad (7.3)$$

$$-i\omega v_{iz} + v_{ix}\frac{dv_0}{dx} = -i\frac{\kappa_z}{\rho_0}\rho_1 - i\frac{\kappa_z B_{oy}}{\rho_0\mu_0}b_y \quad (7.4)$$

$$-i\omega b_x = 0 \quad (7.5)$$

$$-iWb_y = B_{0y} \nabla \cdot \vec{v}_1 \quad (7.6)$$

$$+\mu K_z b_z = 0 \quad (7.7)$$

$$d\rho = C_s^2 d\rho. \quad (7.8)$$

Following the same elimination type procedure as before we obtain a single equation for the z-component of velocity:

$$\frac{d^2 v_{1z}}{dx^2} - \left( K_z^2 - \frac{W^2}{C_M^2} \right) v_{1z} = 0 \quad (7.9)$$

where

$$C_M = (C_s^2 + C_A^2)^{1/2} = \text{magnetoacoustic speed}$$

and

$$C_A^2 = \frac{B_{0y}^2}{\rho_0 \mu_0}.$$

The boundary conditions are

$$v_{1z} \rightarrow 0 \quad \text{as} \quad x \rightarrow \pm \infty.$$

Again we introduce the transformation

$$\xi = K_z x - \Omega$$

and Eq. (7.9) becomes

$$\frac{d^2 v_{1z}}{d\xi^2} - (1 - \mu^2 \xi^2) v_{1z} = 0 \quad (7.10)$$

where

$$\mu^2 = \frac{\mathcal{M}^2}{\kappa^2}$$

$$\kappa^2 = \kappa_z^2 d^2$$

and

$$\mathcal{M} = \frac{V}{C_M}.$$

$\mathcal{M}$  is the "magneto-acoustic" Mach number.

In regions I and III the equilibrium velocity is independent of  $x$  and the differential equation for  $v_{1z}$  can be written as

$$\frac{d^2 v_{1z}}{d\xi^2} - (1 - \mu^2 \xi_{1,2}^2) v_{1z} = 0 \quad (7.11)$$

where

$$\xi_1 = \kappa - \Omega$$

$$\xi_2 = -(\kappa + \Omega).$$

The solutions to Eq. (7.11) satisfying the appropriate boundary conditions are



$$\begin{aligned}
 v_{1z} &= A_1 \exp[-(1-\mu^2 \xi_1^2) \xi] ; \quad \xi > \xi_1 \\
 &= C_3 \exp[+(1-\mu^2 \xi_2^2) \xi] ; \quad \xi < \xi_2.
 \end{aligned}
 \tag{7.12}$$

The matching conditions at the interface are again the continuity of the normal displacement, the normal component of the magnetic field, and the normal stress. With the aid of the continuity equation, Eq. (7.1) these may be expressed in terms of  $v_{1z}$  as

$$\begin{aligned}
 \Delta_{1,2} [v_{1z}] &= -\lambda K v_{1x,1,2} \Delta_{1,2} \left[ \frac{d v_{0z}}{d \xi} \right] \\
 \Delta_{1,2} \left[ \frac{d v_{1z}}{d \xi} \right] &= 0.
 \end{aligned}$$

As was the case with the incompressible flow limit it is now possible to obtain the zero thickness results for this case by considering the  $d \rightarrow 0$  limit of the above equations. Again we must return to the dimensional form of the equations and then take the  $d \rightarrow 0$  limit. Carrying out the matching we obtain the dispersion relation

$$\Omega^2 = \frac{\kappa^2}{\sigma m^2} \left[ \sigma m^2 + 1 \pm \sqrt{4\sigma m^2 + 1} \right].$$

This is in agreement with the results obtained by Fejer (22). In dimensional terms

$$\omega^2 = k^2 c_H^2 [1 + \sigma m^2 \pm \sqrt{1 + 4\sigma m^2}].$$

Again one can see that for unstable cases

$$\sqrt{1 + 4\sigma m^2} > 1 + \sigma m^2$$

the growth rate increases with  $k$ .

For a finite thickness in region II the equilibrium flow velocity is again a function of  $x$  and we must solve Eq. (7.10). A similar equation was obtained by Schuurman (55) for the case of a compressible flow with no magnetic field. The general solution to Eq. (7.10) may be obtained in terms of a series expansion in parabolic cylindrical functions or hypergeometric functions (48, p. 315). However, as was the case with the spheroidal wave equation in the incompressible flow case, the functional series solution is inappropriate for the purpose of discussing the dispersion relation. For this reason we obtain an approximate solution.

In regard to the magnetopause problem we are particularly interested in the region of low velocity just away from the subsolar point. Hence we shall introduce a small "magneto-acoustic Mach number" approximation, i. e.

$$\sigma m^2 = \frac{V^2}{c_H^2} \ll 1$$

This implies  $\mu^2 \ll 1$  provided  $k$  does not become too small. Physically  $\mu^2 \ll 1$  represents a low Mach number approximation for  $k \lesssim O(1)$ , but it may also represent for  $k \gg 1$  a situation where the Mach number is high but finite.

We now use a singular perturbation technique and expand  $v_{1z}$  in terms of the small parameter  $\mu^2$ :

$$v_{1z} = v_{1z}^{(0)} + \mu^2 v_{1z}^{(1)} + \mu^4 v_{1z}^{(2)} + \dots \quad (7.13)$$

Substituting this in Eq. (7.10) we obtain

Zeroth order in  $\mu^2$ : 
$$\frac{d^2 v_{1z}^{(0)}}{d\xi^2} - v_{1z}^{(0)} = 0$$

First order in  $\mu^2$ : 
$$\frac{d^2 v_{1z}^{(1)}}{d\xi^2} - v_{1z}^{(1)} = A_2 \exp(\xi) - C_2 \exp(-\xi)$$

etc.

The solution to the first order in  $\mu^2$  is

$$v_{1z} = A_2 \exp(\xi) \left[ 1 + \frac{\mu^2}{24} (-4\xi^3 + 6\xi^2 - 6\xi + 3) \right] + C_2 \exp(-\xi) \left[ 1 + \frac{\mu^2}{24} (4\xi^3 + 6\xi^2 + 6\xi + 3) \right]. \quad (7.14)$$

For  $\mu^2 \ll 1$  these lead to the dispersion relation:

$$\begin{aligned}
 & 8\kappa \mu^2 \Omega^4 + \Omega^2 \left[ -4 + \mu^2 \left( -1 - 4\kappa + 8\kappa^2 - \frac{16}{3}\kappa^3 \right) \right] \\
 & + (1 - 2\kappa)^2 - \exp(-4\kappa) - \mu^2 \left( \kappa^2 - \frac{4}{3}\kappa^3 \right. \\
 & \left. - \frac{8}{3}\kappa^4 + \frac{8}{5}\kappa^5 \right) = 0.
 \end{aligned} \tag{7.15}$$

For  $\mu^2 = 0$  this relation reduces to that obtained in the hydrodynamic incompressible case. The dispersion relation above is again bi-quadratic but of a complicated form. Numerical solutions have been obtained and the growth rate versus nondimensional wave number is shown in Fig. 9 for various values of  $m^2$ . The zero thickness results are also shown.

The results here show that the finite thickness of the layer does stabilize the short wavelength disturbances which were found to be unstable in the zero thickness limit. Again the growth rate has a finite value for each wave number. Also compressibility effects tend to lower the growth rate of the instability from the incompressible case, and it also reduces the value of the critical wave number  $k_c$ . An expression for  $k_c$  can be obtained from Eq. (7.15) by taking  $\Omega = 0$ . This gives

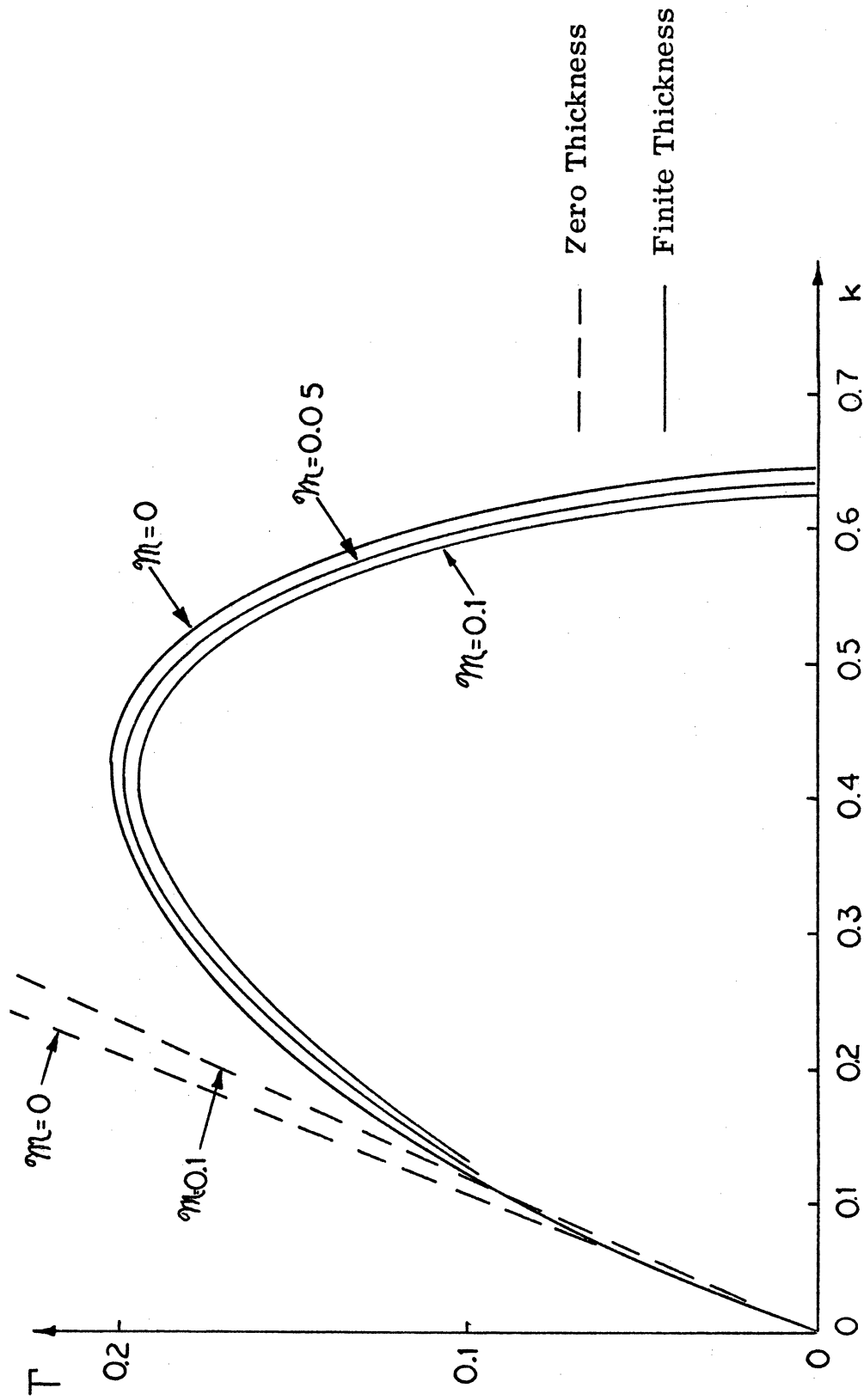


Figure 9. Growth Rate vs Wave Number. Effects of Finite Thickness and Compressibility

$$\begin{aligned} (1-2k_c)^2 - \exp(-4k_c) - m^2 \left(1 - \frac{4}{3}k_c \right. \\ \left. - \frac{8}{3}k_c^2 + \frac{8}{5}k_c^3 \right) = 0. \end{aligned} \quad (7.16)$$

Solutions to this equation for various  $m^2$  are shown in Fig. 10.

Similar results were obtained by Schuurman (55) who studied the finite thickness layer with no magnetic field. The quantitative results he presents, however, are somewhat questionable in the vicinity of  $k_c$  where  $\Omega = 0$ . The difficulty here arises because of the expansion used by Schuurman to solve his dispersion relation.

Returning to the case where a magnetic field is present it can be seen that the presence of a transverse magnetic field does have an effect when the flow is compressible. It increases the growth rate towards the incompressible value. This is so because  $B_{oy} \neq 0$  implies  $C_M > C_s$  and thus  $m^2$  is reduced. Hence in this sense the magnetic field tends to be destabilizing. These latter results agree qualitatively with those obtained when the layer thickness is neglected. For a zero thickness layer Miles (44) found that compressibility effects stabilize the flow, and Fejer (22) showed that a perpendicular magnetic field tends to be destabilizing. However, the zero thickness assumption always leads to increasing growth rate as the wave number increases. When  $m$  is not small,

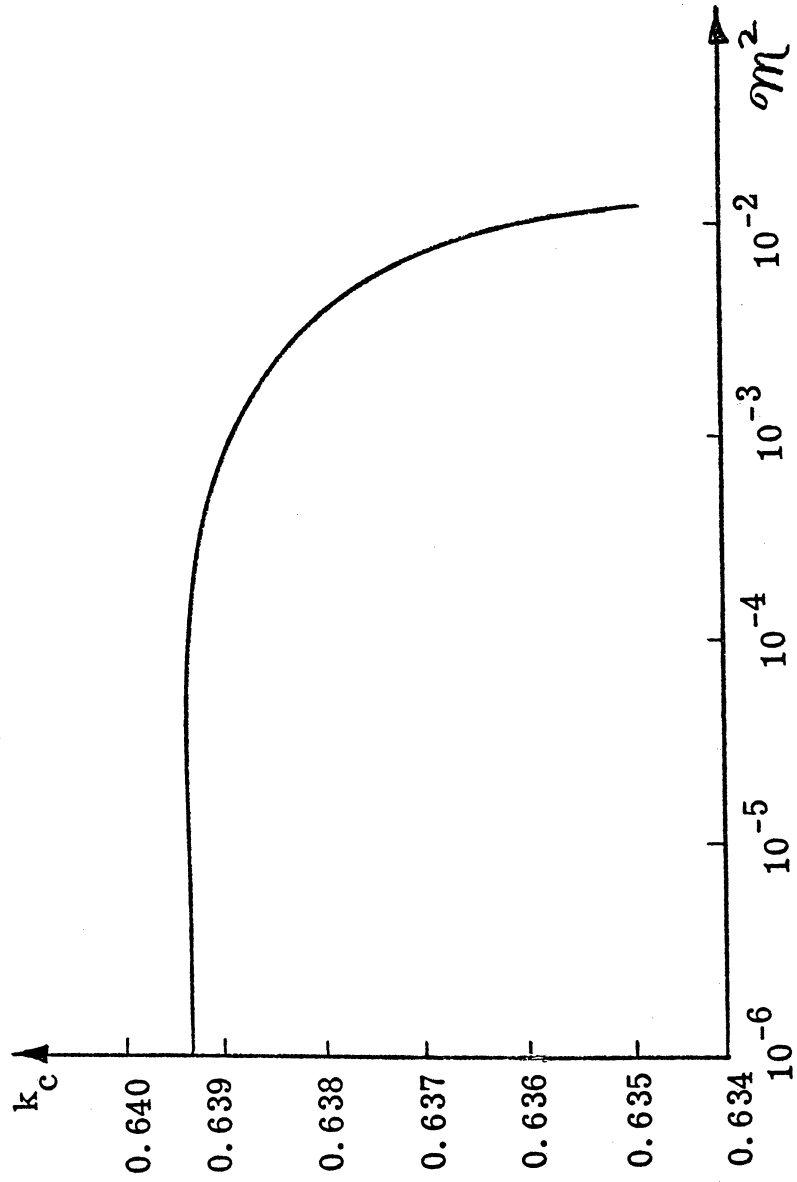


Figure 10. Neutral Stability. Effects of Compressibility and Transverse Magnetic Field

then we must have  $k \gg 1$  for the expansion to be valid. In this case, calculations show that the growth rate is reduced to zero by the finite thickness of the layer although it is not possible to obtain a quantitative growth rate versus  $k$  curve.

As was the case for the incompressible flow, one special case of magnetic field variation is obtainable from the previous results. This is the case of a step function  $B_{oy}(x)$  similar to the step variation of the parallel field discussed in the Appendix. Here no exact solutions are possible, however, and no new results are obtained by considering such a nonphysical variation.

These results, in agreement with Southwood (61), indicate that the low latitude regions of the magnetopause may be unstable. The instability will be characterized initially by the maximum linear growth rate. This growth occurs at a fixed wavelength corresponding to the wave number for the maximum growth rate. This is of the order of ten times the thickness of the shear layer. The real frequency of the growing disturbance also occurs at a fixed value. For the transformed velocity system used here  $\omega_R = 0$ . For a more general flow pattern with  $v_o(x) = V_1$  at  $x = d$  and  $v_o(x) = V_2$  at  $x = -d$  the real part of the frequency is given by

$$\omega_R = \frac{k_z}{2}(V_1 + V_2)$$



Such a linear instability will eventually be stabilized by nonlinear effects either as a finite amplitude quasiperiod wave or as a region of plasma turbulence. The presence of a finite amplitude nonlinear wave would provide a source for the production of wave motion in the magnetosheath and in the outer magnetosphere, and it would provide an explanation of the observed quasiperiodic motion of the magnetopause. Plasma turbulence could also produce wave motion in the magnetosheath and magnetosphere and either of these nonlinear phenomena would provide a means of coupling the solar wind flow with the earth's magnetospheric plasma.

## VIII. SUMMARY AND CONCLUSIONS

In this work we have investigated the Kelvin-Helmholtz, velocity shear, instability in plasma flows with non-zero velocity shear layer thicknesses. The investigation was carried out in the low frequency hydromagnetic range for two types of problems. The first consider the stability of an infinite weakly inhomogeneous slab of two fluid plasma at finite  $\beta$ . An equivalent dielectric tensor approach was used to investigate the local stability of this plasma slab in the very small ion Larmor radius limit. The effect of a varying equilibrium magnetic field as well as an equilibrium density gradient was included in the formulation.

For this case it was found that a shear in the plasma velocity parallel to the equilibrium magnetic field can give rise to an instability in the flow. The growth rate of this instability increases with increasing velocity shear and/or local shear speed, but it was found to decrease with an increasing density gradient. The magnitude of the growth rate remained finite for all wave numbers investigated and was found to reach a maximum value at finite wave number.

Additional work remains to be done in this area if one wishes to know the stability characteristics of the model to all values of wavelength and frequency. In the low frequency regime the stability at

very short wavelengths cannot be determined from the two fluid models considered since it does not include the effects of ion viscosity due to the finite ion Larmor radius. At large wave numbers, small wavelength, these effects become important. A more complete treatment should also consider the effects of wave particle interactions such as cyclotron and Landau damping. To properly treat the above cases a kinetic theory approach, employing the Vlasov equation, should be used. An electrostatic, low  $\beta$ , problem with velocity shear has been treated with this approach by Smith and von Goeler (59). At longer wavelengths, smaller wave numbers, there exists the problem of the applicability of the local approximation to reduce the dielectric tensor to an algebraic form. In this region it may be necessary to treat the differential equation in  $x$  for the perturbed electric field including boundary conditions to completely formulate the eigenvalue problem. Again some work has been done in the low  $\beta$  along these lines by Rosenbluth and Simon (52). They found some special cases for which it was possible to obtain sufficient conditions for stability for the more complex  $x$ -dependent problem.

The second problem investigated was the effect of a finite velocity shear layer thickness on the hydromagnetic Kelvin-Helmholtz instability. For this case the single fluid hydromagnetic equations were

used. The velocity profile through the layer was taken to be linear. Incompressible flows with an arbitrary magnetic field normal to the flow direction and the direction of propagation were studied. Compressibility effects were included for a constant transverse magnetic field. These flow regions approximate the flow field at the magnetopause at low latitudes near the subsolar point. In both cases the finite thickness of the velocity shear layer is shown to stabilize the short wavelength perturbations which were previously found to be unstable in the zero thickness analysis of the problem. Furthermore in the case of incompressible flow the component of the magnetic field perpendicular to the flow velocity and the direction of propagation of the disturbances has no effect on the instability. On the other hand the parallel component of the magnetic field reduces the growth rate of the instability. When the variation of density is taken into account the compressibility effects reduce the growth rate of the instability, but in this case the presence of a perpendicular magnetic field tends to increase the growth rate towards the incompressible value.

For this case a complete linear stability analysis of a hydro-magnetic shear layer may constitute a possible area for additional work. The complexity of the  $x$ -variation of flow and field parameters in the transition region, however, seems to indicate that a

numerical approach to obtain eigenvalues and eigenfunctions for a specific flow configuration will be required. One problem of this specific nature have been treated in the hydromagnetic case by Lessen and Desphande (37-39) who were able to numerically determine the marginally stable modes for a specific problem.

In both of the preceding cases there remains considerable additional work in the area of nonlinear stability. For the two fluid model the complexity of the mathematical model seems to preclude direct treatment of the problem in a manner such as Stix (63) and Weyl and Goldman (71) used for the electrostatic drift wave problem. It may, however, be possible to use a technique such as that of Weinstock and Williams (70) to obtain some information of the nonlinear behavior. For kinetic theory treatment, or regions of instability it may be possible to apply quasi-linear kinetic theory (53). The complexity of the finite  $\beta$  problem may even make this type of treatment impossible, however.

The single fluid hydromagnetic case appears somewhat more accessible to a nonlinear treatment at this time. If one looks at the behavior of a zero thickness shear layer it may be possible to apply an expansion in time near the marginally stable state to investigate nonlinear development. Such a technique was used by Drazin (17) to study the nonlinear hydrodynamic Kelvin-Helmholtz instability

of zero thickness layers with surface tension. Since the presence of a magnetic field produces a "surface tension like" stabilizing effect on the linear problem (11, p. 511), this offers an interesting possibility for a nonlinear treatment of the hydromagnetic problem. Such a technique is based on the "normal mode cascade" expansion of Stuart (65) and Watson (69). This type of work involves two difficulties, however. The first of these is the applicability of only an expansion in time to a system with no characteristic length scale (61). The second involves the difficulty introduced by the magnetic field. For this case the nonlinear flow in the uniform flow regions no longer remains irrotational and both the differential equations and matching conditions become more complicated than the hydrodynamic case.

In conclusion, the presence of non-zero shear layer thickness in the hydromagnetic Kelvin-Helmholtz problem leads to a finite maximum growth rate at a finite wave number for the two cases studied. Short wavelength disturbances found to be unstable for shear layers of zero thickness, with growth rates that increase indefinitely as the wavelength becomes smaller, are stabilized by effects of non-zero layer thickness. Stabilization occurred both in shear layers of infinite thickness and in shear layers where the thickness was finite. The results of the finite thickness study

indicate the magnetopause may be unstable in the low latitude equatorial regions just away from the subsolar point. The instability in this region will be characterized by a finite linear growth rate at a fixed wavelength and frequency. Stabilization of this growth by nonlinear effects presents a source for coupling between the solar wind and the magnetosphere and the generation of wave motion in both the magnetosheath and magnetosphere.

## REFERENCES

1. Anderson, K. A. et al., J. Geophys. Res., 73, 2371 (1968).
2. Aubrey, M. P. et al., J. Geophys. Res., 76, 1673 (1971).
3. Axford, W. I., Quart. J. Mech. and Appl. Math., 13, 314 (1960).
4. Axford, W. I. and C. O. Hines, Can. J. Phys., 39, 1453 (1961).
5. Axford, W. I., Can. J. Phys., 40, 654 (1962).
6. Baikov, I. S., Sov. Phys. — Tech. Phys., 15, 328 (1970).
7. Boller, B. B. and H. L. Stolow, J. Geophys. Res., 75, 31 (1970).
8. Bowers, E. and M. G. Haines, Phys. Fluids, 11, 2695 (1968).
9. Brice, N., J. Geophys. Res., 72, 5193 (1967).
10. Cassen, P. J., Planetary Space Sci., 18, 349 (1970).
11. Chandrasekhar, S., Hydrodynamic and Hydromagnetic Stability, Oxford: Oxford University Press, 1961.
12. Chew, G. F. et al., Proc. Roy. Soc. (London), A236, 112 (1956).
13. Coleman, P. J., "Turbulence, Viscosity, and Dissipation in the Solar Wind Plasma," Proc. Symp. on Turbulence in Fluids and Plasmas, Brooklyn, N. Y.: Polytechnic Press, 1968.
14. D'Angelo, N., Phys. Fluids, 8, 1748 (1965).
15. D'Angelo, N. and S. von Goeler, Phys. Fluids, 9, 309 (1966).
16. Drazin, P. G. and L. N. Howard, "Hydrodynamic Stability of Parallel Flow of Inviscid Fluid," Advances in Applied Mechanics, Vol. 9, New York: Academic Press, 1966.
17. Drazin, P. G., J. Fluid Mech., 42, 321 (1970).
18. Duhau, S. et al., Phys. Fluids, 13, 1503 (1970).



19. Dungey, J.W., Phys. Rev. Lett., 6, 47 (1961).
20. Dungey, J.W. and D.J. Southwood, Space Sci. Rev., 10, 672 (1970).
21. Eviatar, A. and R.A. Wolf, J. Geophys. Res., 73, 5561 (1968).
22. Fejer, J.A., Phys. Fluids, 7, 499 (1964).
23. Gerwin, R.A., Rev. Mod. Phys., 40, 652 (1968).
24. Gotoh, K., J. Phys. Soc. Japan, 16, 559 (1961).
25. Gotoh, K., J. Phys. Soc. Japan, 25, 1178 (1968).
26. Gotoh, K. and T. Numata, J. Phys. Soc. Japan, 27, 764 (1969).
27. Greenstadt, E.W. et al., J. Geophys. Res., 72, 3855 (1967).
28. Hans, H.K., Nuclear Fusion, 8, 89 (1968).
29. Hess, W.N., The Radiation Belt and Magnetosphere, Waltham, Mass.: Blaisdell Publishing Co., 1968.
30. "IBM Application Program," System/360 Scientific Subroutine Package (360 A-CM-03x) Version III, Programmer's Manual, H20-0205-2, White Plains, N.Y.: IBM, Technical Publications Dept., 1968.
31. Jassby, P.L. and F.W. Perkins, Phys. Rev. Lett., 24, 256 (1970).
32. Jokipii, J.R. and L. Davis, Jr., Astrophys. J., 156, 1101 (1969).
33. Karlson, E.T., J. Geophys. Res., 75, 2438 (1970).
34. Kaufmann, R.L. and A. Konradi, J. Geophys. Res., 74, 3609 (1969).
35. Krall, N.A., "Drift Waves," Advances in Plasma Physics, Vol. 1, (Simon and Thompson, ed.), New York: Interscience Publishers, 1968.
36. Lerche, I., J. Geophys. Res., 71, 2365 (1966).

37. Lessen, M. and N. V. Desphande, Phys. Fluids, 9, 1960 (1966).
38. Lessen, M. and N. V. Desphande, Phys. Fluids, 9, 1965 (1966).
39. Lessen, M. and N. V. Desphande, Phys. Fluids, 10, 1968 (1965).
40. MacKenzie, J. F., Planet. Space Sci., 18, 1 (1970).
41. Macmahon, A., Phys. Fluids, 8, 1840 (1965).
42. Melchior, H. and M. Popovic, Phys. Fluids, 11, 458 (1968).
43. Michalke, D. H., J. Fluid Mech., 19, 543 (1964).
44. Miles, J. W., J. Fluid Mech., 4, 538 (1958).
45. Montgomery, D. C. and D. A. Tidman, Plasma Kinetic Theory, New York: McGraw-Hill Book Co., Inc., 1964.
46. Montgomery, D. C., Phys. Fluids, 13, 1401 (1970).
47. Morse, P. M. and H. Feshbach, Methods of Mathematical Physics, Vol. I, New York: McGraw-Hill Book Co., Inc., 1953.
48. Murphy, G. M., Ordinary Differential Equations and Their Solutions, Princeton, N. J.: D. Van Nostrand Co., Inc., 1960.
49. Nakata, I., J. Phys. Soc. Japan, 29, 1619, (1970).
50. Rayleigh, J. S., "On the Stability, or Instability, of Certain Fluid Motions," Scientific Papers, Vol. 1, New York: Dover Publications, 1964.
51. Reviews of Geophysics, Vol. 7 (1969).
52. Rosenbluth, M. N. and A. Simon, Phys. Fluids, 8, 1300 (1965).
53. Sagdeev, R. Z. and A. A. Galeer, Nonlinear Plasma Theory, New York: W. A. Benjamin, Inc., 1969.
54. Scarf, F. L., "Plasma in the Magneto-sphere," Advances in Plasma Physics, Vol. 1, (Simon and Thompson, ed.), New York: Interscience Publishers, 1968.

55. Schuurman, W., Rijnhuizen. Report 69-55, Jutpaas, Netherlands (1969).
56. Sen, A. K., Planet. Space Sci., 13, 131 (1965).
57. Sen, A. K., J. Geomagnetism and Geoelectricity, 20, 225 (1968).
58. Sen, A. K., J. Geomagnetism and Geoelectricity, 20, 245 (1968).
59. Smith, C.G. and S. von Goeler, Phys. Fluids, 11, 2665 (1968).
60. Smith, E. J. and L. Davis, Jr., J. Geophys. Res., 75, 1233 (1970). (1970).
61. Southwood, D. J., Planet. Space Sci., 16, 587 (1968).
62. Stewartson, K., "Aspects of Nonlinear Stability," Seminar, The University of Michigan (1970).
63. Stix, T. H., Theory of Plasma Waves, New York: McGraw-Hill Book Co., Inc., 1962.
64. Stix, T. H., Phys. Fluids, 12, 627 (1969).
65. Stuart, J. T., J. Fluid Mech., 9, 353 (1960).
66. Syrovatskii, S. I. (1953). These results are given as a problem in Electrodynamics of Continuous Media by L. D. Landau and E. M. Litshitz, p. 228, Reading, Mass: Addison-Wesley Publishing Co., 1960.
67. Talwar, S. P., J. Geophys. Res., 69, 2707 (1964).
68. Tannenbaum, B. S., Plasma Physics, New York: McGraw-Hill Book Co., Inc., 1967.
69. Watson, J., J. Fluid Mech., 9, 371 (1960).
70. Weinstock, J. and R. H. Williams, Bulletin American Physical Society, Series II, 15, 1443 (1970).

71. Wegl, G. and M. Goldman, Phys. Fluids, 12, 1097 (1969).
72. Wolfe, J. H. and D. S. Intriligator, Space Sci. Rev., 10, 511 (1970).

## APPENDIX

In this appendix we will discuss two special cases of the incompressible flow limit. The physical basis of these cases is not as firm in application to the magnetopause problem but the results are interesting and easily obtainable from the basic model of Sections V and VI. These cases are oblique propagation with zero transverse field and a step variation of the parallel field.

### 1. Oblique Propagation with Zero Transverse Magnetic Field

In this case we take  $B_{oy} = 0$ . We now consider  $k_y \neq 0$ . Following the same procedure as was used in Section VI we obtain:

$$\begin{aligned} & \Omega^4 + \Omega^2 \left\{ \frac{K_z}{K} K - 2K \left(1 + \frac{1}{A^2}\right) - \frac{K_z^2}{4K^2} [1 - \exp(-4\frac{K}{K_z})] \right\} \\ & + K^4 \left(1 - \frac{1}{A^2}\right)^2 - K^3 \frac{K_z}{K} \left(1 - \frac{1}{A^2}\right) + \frac{K^4}{4} \frac{K_z^2}{K^2} [1 - \exp(-4\frac{K}{K_z})] \\ & = 0 \end{aligned} \tag{A.1}$$

where  $K^2 = k_y^2 + k_z^2$ . Squire's theorem (38) applies for this case and the maximum growth rate occurs for  $k_y = 0$ . This case is exactly the same dispersion relation as the case for  $B_{oy} \neq 0$  discussed earlier. The results are the same as those shown in Fig. A-1.

## 2. Step Variation in Parallel Magnetic Field

The second special case considers a crude method for considering variations in  $b_0$ . This is applicable to the magnetopause case discussed first or the special case discussed above. From Eq. (6.13) and its solutions can be seen that each is a solution in a local region, i.e. region I, II, or III. The solutions are properties only of conditions single region. Thus one general way of considering a variation of  $b_0$  is to take  $b_0$  constant but a different constant in each region.

For this case we can write the solutions to Eq. (6.13) as

$$\begin{aligned} \delta &= A_1 e^{-\xi} && ; \xi > \xi_1 \\ &= \frac{A_+ e^{+\xi}}{(\xi^2 - \alpha_+^2)^{1/2}} + \frac{A_- e^{-\xi}}{(\xi^2 - \alpha_-^2)^{1/2}} && ; \xi_2 < \xi < \xi_1 \\ &= C_3 e^{+\xi} && ; \xi < \xi_2. \end{aligned}$$

The jump conditions now become

$$\begin{aligned} \Delta_{1,2} [\delta] &= 0 \\ \Delta_{1,2} \left[ (\xi^2 - \alpha_j^2) \frac{d\delta}{d\xi} \right] &= 0. \end{aligned}$$

In the above  $\alpha$  will take a different value in each region. For this case of jump variations in  $b_0$  one set of  $b_0$  variations leads to an exact

solution for the problem. An exact solution is obtained if region II is considered an infinitely conducting current sheet such that

$b_{o2} = 0$ . For this case  $\alpha_2 = 0$  and  $\vec{k} = k_z \hat{e}_z$  and the WKB approximation reduces to the exact solution

$$\delta = \frac{A_+ e^{+\int}}{\int} + \frac{A_- e^{-\int}}{\int}.$$

Matching conditions of the interfaces for a z-component field reversal across the interface ( $b_{o3} = -b_{o1}$ ) leads to the dispersion relation:

$$\begin{aligned} & \Omega^4 + \Omega^2 \left\{ \kappa(1-2\kappa) - \alpha^2 - \left[ \frac{1 - \exp(-4\kappa)}{4} \right] \right\} \\ & + (\kappa + \alpha^2)^2 \left[ \frac{1 - \exp(-4\kappa)}{4} \right] + \kappa^2 (\kappa^2 - \kappa - \alpha^2) = 0. \end{aligned} \quad (\text{A. 2})$$

This equation is valid for any value of A. Numerical solutions were obtained for this equation and are shown in Fig. A-1. For this very special case one can see that the qualitative features of the approximate model, the existence of a  $k_c$  and the reduction in the maximum growth rate for all A, agree with the quantitative results of the exact solution. For  $b_{o2} \neq 0$  approximate solutions can also be obtained by use of the WKB technique. Solutions of this type show the same qualitative behavior as those discussed above.

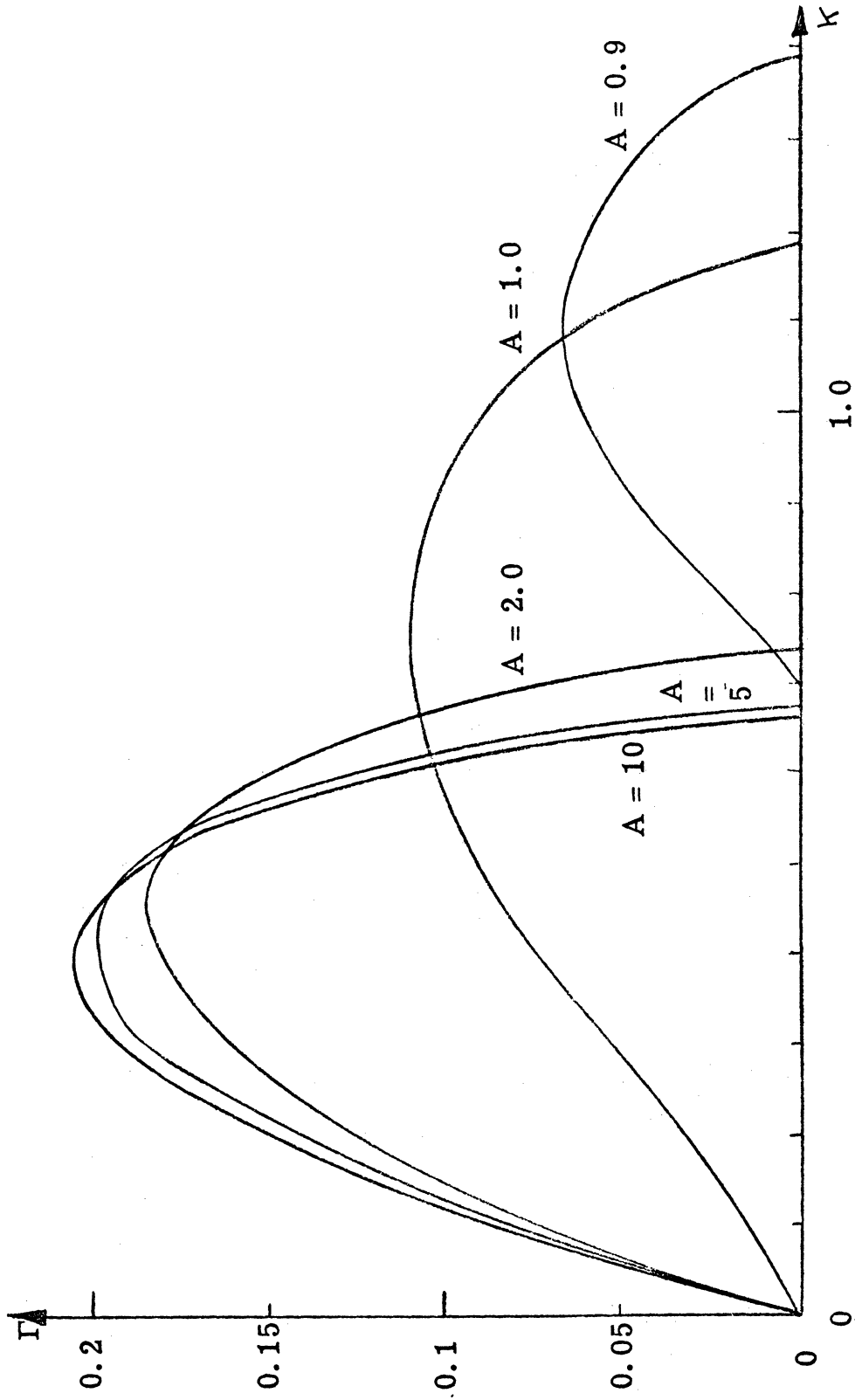


Figure A-1. Growth Rate vs Wave Number. Exact Solution for No Magnetic Field Inside the Layer



DOCUMENT CONTROL DATA - R & D

(Security classification of title, body of abstract and indexing annotation must be entered when the overall report is classified)

1. ORIGINATING ACTIVITY (Corporate author) The University of Michigan Ann Arbor, Michigan		2a. REPORT SECURITY CLASSIFICATION Unclassified	
		2b. GROUP	
3. REPORT TITLE Hydromagnetic Kelvin-Helmholtz Instability in Shear Layers of Non-Zero Thickness			
4. DESCRIPTIVE NOTES (Type of report and inclusive dates) Technical Report			
5. AUTHOR(S) (First name, middle initial, last name) R. S. B. Ong and N. F. Roderick			
6. REPORT DATE May 1971		7a. TOTAL NO. OF PAGES 97	7b. NO. OF REFS 72
8a. CONTRACT OR GRANT NO. AF-AFOSR-825-67		9a. ORIGINATOR'S REPORT NUMBER(S)	
b. PROJECT NO.			
c.		9b. OTHER REPORT NO(S) (Any other numbers that may be assigned this report)	
d.			
10. DISTRIBUTION STATEMENT Qualified requesters may obtain copies of this report from DDC.			
11. SUPPLEMENTARY NOTES		12. SPONSORING MILITARY ACTIVITY	
13. ABSTRACT The hydromagnetic Kelvin-Helmholtz instability is investigated for velocity shear layers of non-zero thickness. Two cases are studied in the low frequency hydromagnetic regime. The first case considers an infinite weakly non-homogeneous two fluid plasma in the finite $\beta$ limit with the shear flow parallel to the equilibrium magnetic field. The second case considers a velocity shear region of finite thickness. Criteria for instability are found for both cases. The effect of the compressibility of the fluid on the instability is also discussed.			

14. KEY WORDS	LINK A		LINK B		LINK C	
	ROLE	WT	ROLE	WT	ROLE	WT
hydromagnetic Kelvin-Helmholtz shear layer instability non-homogeneous plasma finite thickness layer growth rate						

